University of South-Eastern Norway

www.usn.no

FMH606 Master's Thesis 2022

Industrial IT and Automation

Real-time monitoring of train wheels and track conditions based on acoustic measurements and multivariate data analysis

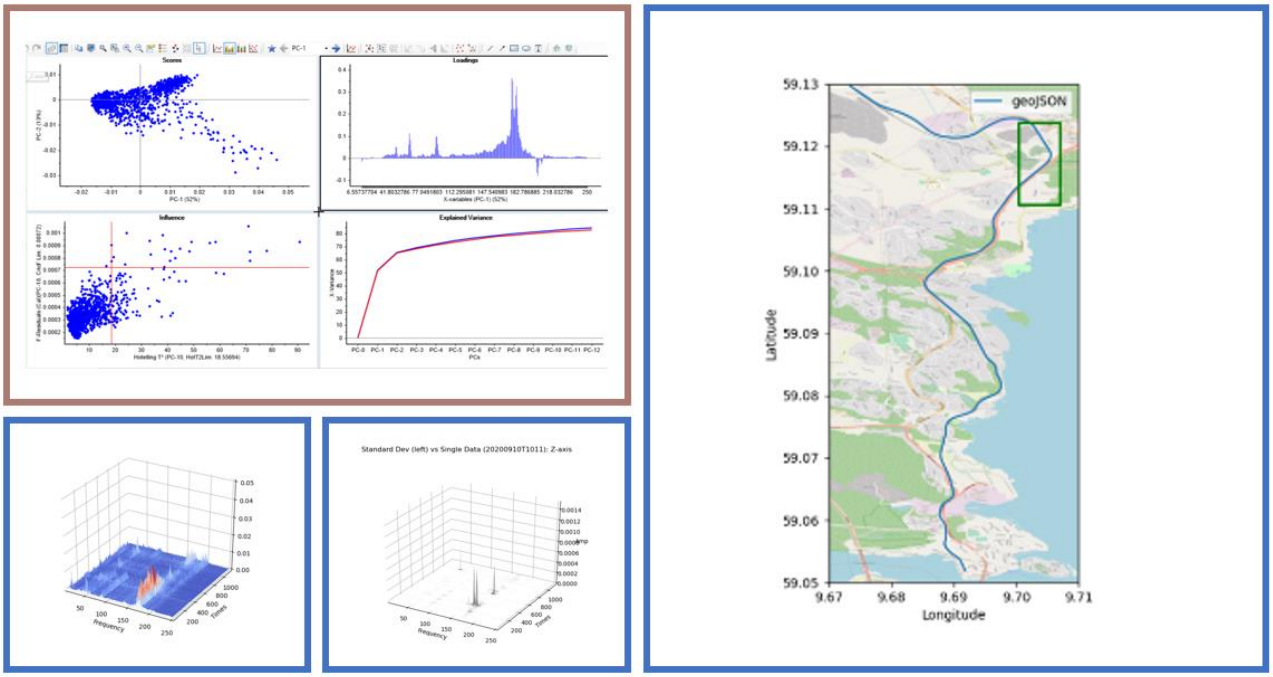

Dilruba Tariq Jinia
238753

University of South-Eastern Norway

www.usn.no

Course: FMH606 Master's Thesis, 2022

Title: Real time monitoring of train wheels and track conditions based on acoustic measurements and multivariate data analysis

Number of pages: 63

Keywords: chemometrics, pca, acoustic sensing, acoustics , fft, multivariate

Student: Dilruba Tariq Jinia, 238753

Supervisor: Maths Halstensen

External partner: CEMIT Digital AS

Summary:

With rail-vehicle transport considered as greener and more sustainable means of travel in recent global times, there is a need for study and exploration of a real-time monitoring system for rail and its vehicle structures, that can facilitate identification of track defects and the vehicle's structural monitoring. The method proposed for this is acoustic chemometrics, is a data-driven approach, where acoustics, or vibrational data is collected across three orthogonal axes and analyzed for structures or patterns that can suggest and/or indicate any faults or irregularities as can validate some of the hypotheses proposed by from Cemit.

With an objective to understand and apply the mechanism of acoustic chemometrics for such purposes, pre-existing acoustic data from Cemit's data collector has been used. The accelerometer data was converted from time-domain to frequency domain, and plotted across a spectrum to have an initial understanding of the dominant frequencies at play.

Based on visual observations of the existing dominant frequencies, unusual or interesting spots along the original track of Brevikbanen, which was the track used for experiment, was suggested for deeper analysis. An initial chemometric analysis on averaged spectra was performed as an exploratory analysis, and modifications were suggested for more productive and specific chemometric analysis. The need for more experiments to produce reference data is also talked of, and a brief review of few studies that has worked with modelling and simulating track defects and rail-wheel interactions were also brought into light.

Preface

The presented master's thesis is written as a requirement in the final course of FMH606 Master's Thesis, accounting for 30 credits of the master's degree program in Industrial IT and Automation. This study can be sought as a continuation of FM4017 Project of the same study program, where the focus is now more into the analysis of already available accelerometer data from Cemit Digital Collector (CDC)'s IMU unit, and conditioning of the raw data into meaningful analytical sonograms to be studied for chemometric analysis.

The main purpose of undertaking the research is to establish, or investigate in the least, the potential of acoustic chemometrics analysis to see if the acoustics recorded of a moving rail vehicle can help substantiate hypothesis proposed by Cemit (see Appendix A).

While numerous studies are already done on vibrational data pertaining to rail tracks, most of which have used the acoustics data from sleepers, or rails to monitor soil conditions, or in identifying signature soundscapes in an off-line, controlled settings. The territory of research done to use real-time vibration data on a train body, which should ideally have more useful real-time, dynamic information, is rather uncharted, leaving vast potentials left for discovery.

Cemit's initiative to encourage this area of research is commendable, and with proper results and further encouragement, could result in innovative and novel methods unthought of in business areas of rail monitoring.

My sincerest gratitude is towards the company, and to all the involved team members who have helped me with resources, cooperation and their own knowledge whenever requested.

I would also like to thank my supervisor, Maths Halstensen, for redirecting and guiding me during many challenging parts of the research, and for always being supportive for any progress I have made during the semester-long thesis.

I finally add an extended gratitude to all the employees at Cemit for being extremely welcoming, supportive, and refreshing, during the rather few handful hours I got to spend with them while studying in Cemit's office premises.

Dilruba Tariq Jinia, ID -238753

Porsgrunn, 18th May 2022

Contents

List of Abbreviations

DAQ – Data Acquisition

CDC – Cemit Data Collector

IMU – Inertial Measurement Unit

GPS – Global Positioning System

MEMS – Micro Electro-Mechanical System

FFT – Fast Fourier Transform

MVA – **M**ulti**v**ariate Data **A**nalysis

AC – Acoustic Chemometrics

PC – Principle Component

PCA – Principle Component Analysis

List of Figures

1 Introduction

This chapter starts with a background that provides context from previous research around this area, followed by problem definition, which essentially is the question that this study attempts to answer. Then presented are the purpose and objectives, detailing any goals achieved that are fruitful to the problem at hand.

Scopes and limitations are also included in this section, which will describe the area and boundaries within which the study is done. The final subchapter will explain the thesis structure, which will mainly be the outline of the paper.

1.1 Background

There is a rise in awareness of the fact that rail transport is becoming more prevalent as a regular means of passenger commute, material transport between facilities, export, import, and more recently, the remarkable idea of working out a rail management system [1] that can enable passenger travel spanning national borders without worrying about signaling system compatibilities.

This uprise in demand, and the realization that rail transportation is favored as a sustainable, greener and more carbon-friendly public transportation of choice[2], has also drawn more invested research towards subjects related to it now more than ever. Anticipating the growing traffic rates, and the stress undertaken by the currently existing rail structure and soil structures, several studies have emerged to propose analysis of acoustic data collected from train, rail, and soil structures in attempts to find correlation amongst rail conditions and the underlying frequencies[3]. Accelerometers are almost always the preferred sensor, compared to alternatives such as geophones[4] or microphones, and have been found to be the standard sensor type for studying vibrational data on any sort of rail or rail vehicle structures.

Related Studies:

Frequency analysis, performed from acquiring acoustic measurements mounted on sleepers and the rail, can be analyzed for effects of dynamic load on sub-soil structures[5], as found by a foundational master thesis work at NTNU. The analysis showed expected change in eigenfrequencies in correlation to different soil conditions along two extreme periods of weather in a year.

Analysis of vibrational acceleration data gathered from sleepers and the lying rail structure were also studied for seasonally frozen regions[3]. Dynamic and experimental modelling methods have been performed using tri-axial accelerometers attached on wheel to study noises that occurs due to wheel and flanges passing a curve [6], and on bogie side frames of freight car to study rail defects using wavelet based algorithm[7], although these studies and experiments were either done in very controlled environments with fixed track or bogie lengths, and/or inside roller test rigs. These studies are very specialized towards working with particular aspects of rail-wheel analysis, and can help provide explanations and basis for the findings that may emerge from this thesis.

1.2 Problem Definition

In order to model the aspects of rail wheel interaction, which is very essential in understanding how rolling stock affects rail structure over time, a good comprehension of the dynamics relating to the forces acting on the rail surface and the wheel contact surface are important to achieve. While many studies have tried to answer questions about these interaction dynamics using mathematical modelling and often expensive controlled experiments, a head-on approach to analyzing the frequency changes in presence of multivariate, natural external forces and noise could be much more desirable.

Cemit is a digital solutions company that aims to pioneer in building viable rail monitoring technology that considers future advancements by exploiting the numerous amounts data it gathers using its own sensor-DAQ unit called the CDC. As such, Cemit, wants to explore the idea of investigating various of its hypothesis (Appendix A) - many of which suggest amplitude variations in vibrational data in drawing out track defects and wheel conditions - using a rather data-driven approach, where acoustic data gathered from a chosen subject vehicle can be analyzed over the course of various runs to understand where to look for information that says something about the condition of the rail and the vehicle infrastructure.

1.3 Purpose and Objectives

The purpose of this study is to analyze the acoustic measurements from already gathered accelerometer data of a freight train body running along Brevikbanen, in order to observe the frequencies that surmise while the freight vehicle rolls on the rail track. An observation of a changing of these frequencies is expected to reveal more information about important areas to look into for further specific data harvesting and analysis – with a goal to validate the proposed hypotheses.

Given the accelerometer data available from IMU and location co-ordinates from GPS, the goals are to-

- Analyze, study and establish common frequencies that are dominant along various ranges in frequency spectrum, in all three axes (transverse, longitudinal and vertical)
- Investigate deviation in amplitudes of frequencies compared to an averaged, representative frequency spectrum specific to the rail route, serving as a reference start
- Explore relationship between the train's velocity and from frequency spectra to identify or suggest features or specific areas as candidates for multivariate analysis
- Perform a preliminary multivariate analysis, namely PCA, to interpret and evaluate the findings on the scores and loadings

The outcomes of the objectives have no specifics yet, but is to be determined based on the findings from the analysis. However, a fruitful study would help establish, in the least, the ability of chemometric analysis in explaining some the variation in acoustics of a given vehicle running on the same rail route.

1.4 Scope and Limitations

The study is done using data collected from a single subject vehicle, namely Skd 22[8], a shift tractor with suitability for tunnel work purposes. A picture of the vehicle taken by Cemit's personnel, is shown in Figure 1.1.

The data is collected over the track of Brevikbanen, which runs routinely between the limestone quarry in Porsgrunn and Norcem's cement factory at Brevik, and is the only track that data is available for. The extent of study and analysis applied to it are constrained to this subject vehicle and the track.

This thesis was undertaken in co-operation with Cemit, in order to provide insightful approach to the concept of real-time analysis using accelerometer data - a system which was proposed in a prior project study. The data acquisition methods for this thesis, however, vary in certain manners, such as pre-processing of raw data, where, in past methodology, pre-processing measures such as amplification and filtering were possible for modification.

It should also be noted that the initial plan to conduct field experiments with custom-ordered accelerometers by Cemit, for exactly this study, were delayed due to the understandably occupied schedule of personnel, whose presence and assistance were a must for initiation and conduction of such field experimentations.

Figure 1.1 Subject vehicle, a 1972 Skd 226, weighing 32tonnes (without carriages)

Therefore, past data from the company's own device, commonly called the CDC, is used to proceed with the study. Using just historical data has its limitations of course, many of which has contrived the quality and extent of the analysis. Additional data, for example, regarding the structure of the vehicle, weight of material it carries during the experiments, and a visual inspection of parts of the track in Brevikbanen – are some of the freedom new experimentations could allow that historical data wouldn't.

And hence, the following limitations relevant to this study are reminded :

- The analysis is only applicable for the subject vehicle, and could be applied with more versatility if subject vehicle type and factor could be experimented with.
- As the duration of this thesis is also subject to time constraints, study and analysis were continued with past data, and potential to conduct new experiments were not regarded after a certain period. Data analysis is thus applicable for only rail and vehicle

conditions of that time

- Since sampling rates and conduction of test experiments to analyze various scenarios proposed by hypotheses were not available for moderation, the available data was utilized for analysis to the best of knowledge and with time constraints as reminders.

1.5 Thesis Structure

This thesis report is structured to provide the reader with relevant, yet simplified theory and background knowledge of the concepts connected to the analytical aspects of acoustic monitoring and chemometrics. The aims, constraints, purpose, and objectives have been introduced, with a brief preface to some of the related work done on similar topics, to acclimatize the reader to a proper context before diving into the technical chapters.

Methodology has been reserved in a single chapter that explain the tools, software, and walkthroughs on how to arrive at results. Results and analysis are separated into two chapters, so the results are viewable in a single section. The analytical process used in this study have no concrete start to finish, so much of this is addressed in a much-needed Discussion chapter, after which a short conclusion and some suggestions to carry future research work is provided

2 Theory

This chapter aims to provide background on the working principle of the sensors used for the acoustic measurements, relevant frequency analysis of the time-domain data, and a related brief literature study to assist in the interpretation and understanding of the patterns revealed in the frequency domain.

2.1 Accelerometers

Accelerometers are quoted to be among the "legacy micro electro-mechanical systems from early years"[9], and is the preferred sensor for measuring the rate of change of movement of a body it is attached to. The working principle of an accelerometer can be depicted using a simple model of a second-order spring-mass system essentially forming a well-known oscillator[9], visualized in Figure 2.1.

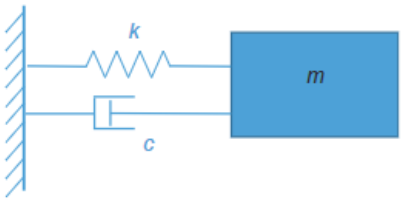

FIGURE 45.1 Schematic model of a second order spring–mass system.

Figure 2.1 A spring-mass-damper model [9, p. 880]

Where ***k*** is the spring stiffness, ***c*** is the damping co-efficient, which is considered, since the oscillations measured on a rail vehicle are not expected to last forever without resistive forces.

The differential equations that model the dynamics are of second order, and considers the damping co-efficient, however, a deeper dive of the entire system of equation[9, p. 880], but the details of these are perhaps not essential for a rudimentary understanding of accelerometers at this point.

In consistence with the physical principles of Hooke's Law, the spring will manifest a restoring force proportional to the amount that us stretched or compressed[10], and that force can be calculated using the Equation 1.1:

$$F = kx \tag{1.1}$$

or,

$$F \propto x \tag{1.2}$$

indicating that a higher force will be exhibited by the spring with higher displacement. Given Newton's second law of motion, $F = ma$, and equating the forces from Equation 1.1, the following is justified:

$$ma = kx \tag{2.3}$$

$$a = \frac{kx}{m} \tag{1.4}$$

where,

a = acceleration of mass attached to spring,

revealing the rate of change of a body's movement in terms of its mass, measuring the vibration of the body.

This principle can be adapted to create MEMS of various mechanisms, and the one used in CDC is that of electrical capacitance. Capacitive accelerometers are preferred for monitoring large structures because of their ability to detect measurements across a wide frequency rage while maintaining good stability compared to other mechanisms[11], piezoresistive ones for example.

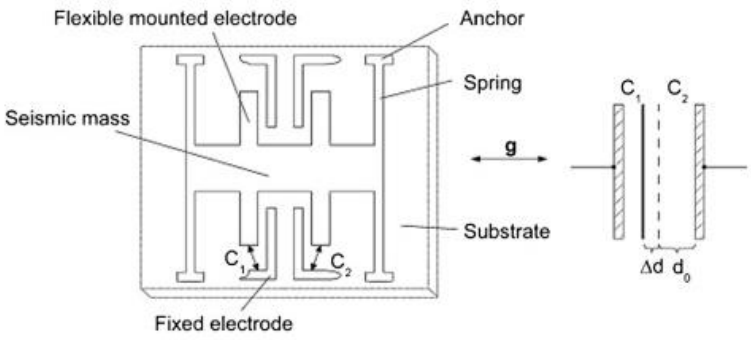

Figure 2.2 Capacitive accelerometer principle demonstrated

Figure 2.2 shows a good depiction of the mass-spring-damper system adapted as a capacitive accelerometer, with a stationary plate and a secondary freely-moving plate connected to the measured mass-body, forming a capacitor[12]. The capacitance detected is a function of the distance *d* between these plates, and later converted to output in electrical volts.

2.2 Frequency Analysis of Time Series Data

Why analyze frequency spectrum?

When measuring time-series data, accounting for the frequency components of a signal can be difficult from just looking at the time-domain information. Analyzing noise, for example, would be challenging from just looking at a time-domain signal, while the same signal displayed on a frequency spectrum would show prominent and noisy amplitudes with much more clarity, an exhibit shown from a collected example online on Figure 2.3.

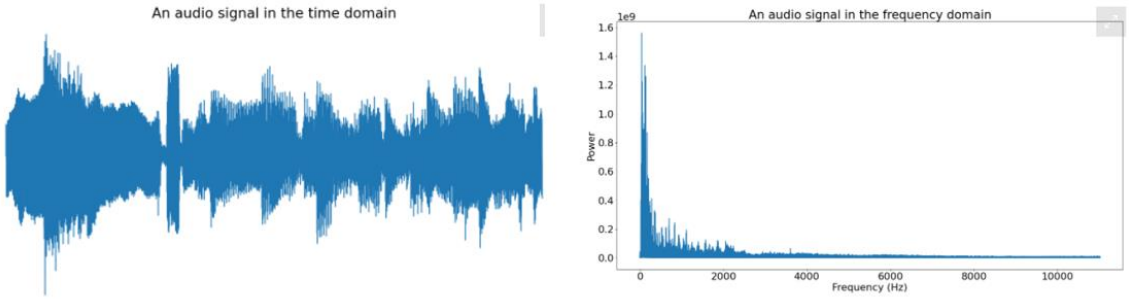

Figure 2.3 Time-domain vs Frequency-domain representation of signal [collected]

Plus, for systems and processes where particular frequency components carry or reveal important information about states of that system, it becomes important to monitor the spectrum to understand the signals along the time domain.

2.2.1 Fast Fourier Transform (FFT)

The Fast Fourier Transform (FFT) is such an algorithm that allows calculation of the frequencies for a discretized time window of the signal, an operation known as Discrete Fourier Transform or DFT[13], but in a computationally efficient manner. The FFT is very prevalent in its use for spectral frequency analysis, and is conceptually intuitive to understand in its mechanisms.

The following terms and parameters are introduced to understand parameters used in generating spectrograms.

Parameters for FFT:

Sampling rate (S_r): Time series data are discretely sampled at a fixed sampling rate per second, hence denoted in Hertz, Hz. Sampling rate (S_r) is chosen considering Nyquist Theorem for sampling, which states that sampling rate has to be double the maximum frequency component being sampled[14]. Therefore,

$$S_r = 2 \times F_{max} \tag{1.5}$$

where,

$$F_{max} \text{ is the maximum sampled } frequency$$

Window size (*n*): window size is selected in number of samples, and determines the duration of time window on which FFT is performed. For ***n*** number of samples, the duration of the window, denoted as $T(n)$ is thus:

$$T(n) = n * T(N) \tag{1.6}$$

or,

$$T(n) = n * 1/S_r \tag{1.7}$$

where,

$T(N)$ is the period of the signal, assuming N is the total number of samples in 1 second.

Depending on the frequency component wished to be sampled, the window size should be adjusted. If high frequencies are to be sampled, window size should be smaller, which results in smaller time duration of that window size and hence, higher frequencies captured. The duration of the window size is also known as the '**time resolution**' or T_r, is essentially the duration analyzed for FFT as a time.

Frequency resolution(F_r): the frequency band of a 'bin'

Bins: a bin is a single band of frequency, or unit frequency in an FFT. If an FFT is divided into more bins, the resolution in increased for that FFT, in other words, the more precise and less truncated the FFT peaks are.

A bin can be equal to or less than the window size, n. Bins are usually in powers of 2.

While T_r is a duration of the length of signal analyzed for FFT, $\boldsymbol{F_r}$ is the precision of that the FFT is plotted with. F_r and T_r are inversely proportional, and F_r can be found by just inversing T_r.

F_r can found by-

$$F_r = \frac{1}{T_r} = \frac{1}{\frac{n}{S_r}} = \frac{S_r}{n} \tag{1.8}$$

or,

$$F_r = \frac{F_{max}}{no.of\ bins} \tag{1.9}$$

However, the window size is usually too large for the number of divisions (bins), so smaller intervals are used instead. The number of bins can be half the window size, or smaller. Equation 1.9 is then used to calculate the frequency resolution.

A frequency resolution of 1Hz, for instance, will thus mean that each amplitude plotted in frequency axis will have a width of 1Hz.

An FFT can also have an *FFT Size*, which is essentially defining the FFT in in terms of the intervals or number of bins used to divide FFT. [improve]

Spectral Leakage and Windowing:

When a window is applied to the time signal to obtain the FFT, the period of the original signal sampled may not be in the same period as the window that is analyzing part of that signal. Thus, spectral leakage can arise if the period for FFT and the window size duration are assumed to repeat in exact intervals throughout all time[15]. Figure 2.4 is collected to demonstrate the undesired effect of spectral leakage on the resulting FFT.

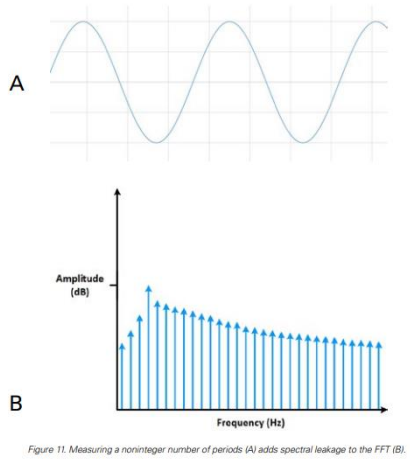

Figure 2.4 Effects of a spectral leakage [16]

A windowing function can prevent spectral leakage due to non-integer number of cycles by tapering the shape of the time window used to perform DFTs. It multiplies the time record by a finite-length window with an amplitude that varies smoothly and gradually toward zero at the edges[16], an example of such a window shown in Figure 2.5.

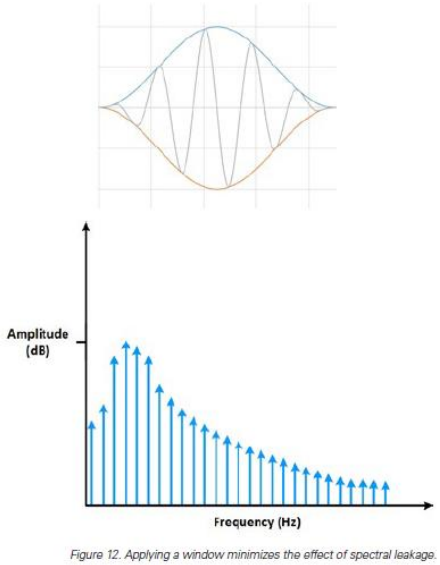

Figure 2.5 Effect of windowing function, collected

There are many window functions, and selecting the appropriate one will depend on how far the freqeucny content can vary from the frequency of interest[16].

2.2.2 Spectrograms

A single FFT displays frequency components for a duration of a time window. For a process where frequency components have to be analyzed along time, the FFTs would have to be stacked consecutively along the time axis, displayed using a spectrogram.

A spectrogram can be 2D, where a color scheme demonstrates the varying power intensity of the signal along the frequency axis, such as one demonstrated in Figure 2.6. A 3D spectrogram would show just the same information, in form of a surface plot, as exhibited by an example from MathWorks's demonstration of the concepts[17]

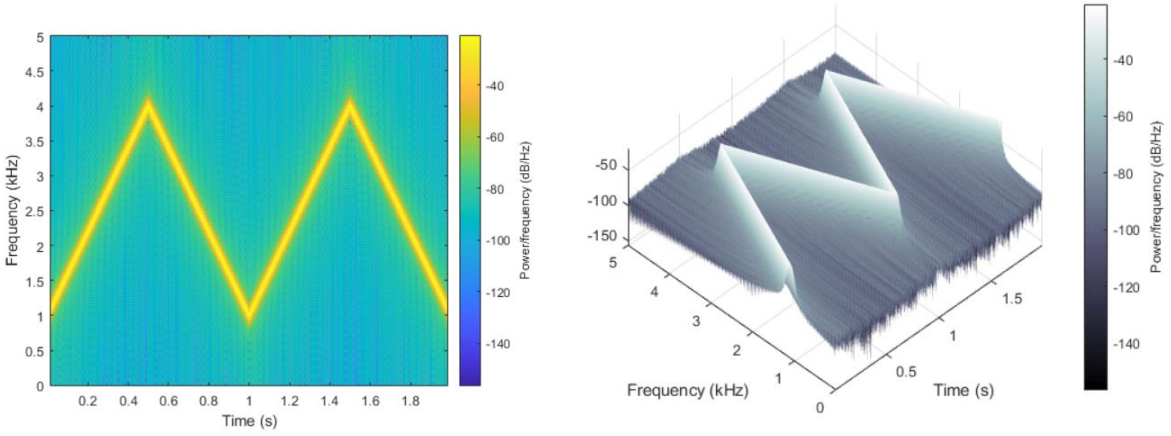

Figure 2.6 (left) A 2D Spectrogram with signal strength depicted using color changes, {right) 3D plot of spectrogram using surface plot

Apart from the required time signal data, spectrograms can take in arguments specifying :

- sampling rate
- window size,
- windowing function and
- the number of samples for overlapping. ***Overlapping*** is done to ensure that the samples at the edge of the time window are weighted higher than the samples mid-window, since applying a window function will reduce amplitude around the edge of the time windows. This ensures minimal loss of information due to windowing functions

Since data pre-processing and treatment are all developed in Python, its SciPy. Signal library is used to generate spectrograms. The function returns the time, frequencies, and the amplitudes to be plotted, in three separate arrays[18].

2.3 Acoustic Chemometrics

The concept of measuring acoustic data without being invasive to the operations of a process or system, and pre-processing of that data to make it suitable for multivariate calibration and data-driven, chemometric analysis, is widely recognized as the term 'Acoustic Chemometrics', or AC. This technique has not only proven suitable for a growing number of industrial and process applications, but also due to its ability to seamlessly utilize multivariable for calibration and modelling quite well.

Figure 2.7 shows an overview of the steps involved in a flow - a popular schematic used often to put into picture the A to Z of the technique.

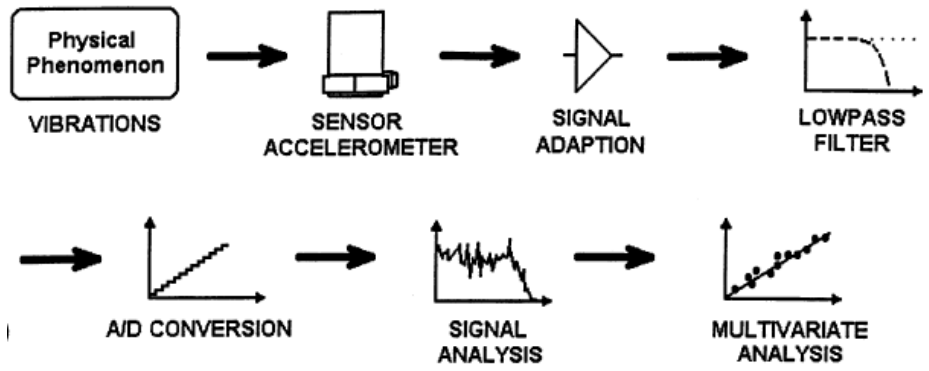

Figure 2.7 General flow and steps involved in Acoustic Chemometrics process[19]

Studies and experiment that have used this approach have seldom had to change this flow, and is therefore applicable for the purposes of this study too. The diagram itself explains the process fairly well, however, since the analysis done on the data for this study is pre-exiting and did not involve carrying out any new experiments, the methodology of this study does not include details of signal adaptation, filtering and A/D conversion. Information and details gathered about these steps, however, shall be included along appropriate, relevant chapters.

Signal Analysis:

Aforementioned FFT and Spectrogram Analysis, available in details in Chapter 2.3, of the acoustic data are the signal analysis performed.

Multivariate Analysis: While multivariate analysis approaches span many algorithms, from unsupervised ones, such as PCA, to supervised methods, such as PCR and PLS-R, the algorithms that this study concerns, given the available data and stage of study, is Principle Component Analysis, PCA.

The next subchapter covers the fundamentals concerning PCA, including the parameters that are used in evaluating the results of PCA.

2.3.1 Principle Component Analysis

Principle Component Analysis is a multivariate analysis approach that can help interpret data visually, help recognize important, recursive patters, while simplifying complexity of the data by reducing the dimensionality.

It does so by reducing the number of variables, ***p***, according to components that explains the highest variance, resulting in reduced number of variables, hence fewer dimensions[20].

Equation 2.4 represents how PCA decomposes multidimensional, multivariate data matrix, X into information in terms of ‘scores’ and ‘loadings’:

$$X = TP' + E \tag{2.0}$$

where,

X is 2D data matrix of size $\boldsymbol{nxp}$, n being the number of samples, and p being number of variables

T is a matrix of the calculated scores of respective Principle Components, and is the same size as X

P is a vector containing the Principle Components, as can at max be of size $\boldsymbol{p}$,

E is the error term, often not included when if data is mean-centered.

Summary of how PCA is performed:

1. Sample data from experiment is plotted in the original variable space. Data is checked to see if any pre-processing is needed.

2. Data pre-processing is then performed, (standardized scaling, mean centering) as seen fit

3. The first PC is calculated in the ***direction of maximum variance***, using the well-known Sum of Least Squares method. A PC, compared to a p-variable, is then actually a linear combination of the original set of p-variables.

4. The second PC (equation of a straight line) is calculated orthogonal to the first PC, in direction of second, and continues on for the rest of PCs. The highest possible number of PCs for a dataset is equal to the number of variables, ***p***. The PCs are now linear equations that are orthogonal to each other.

5. Calculated value of each data sample is projected on to the PCs. The projected data values on each PC are now called '***scores'***. The number of scores for each PC is the same as the original number of data points

6. The co-efficients that make up the linear equation of each PC are then called '***loadings'*** for that PC.

7. The ***score plots*** and the ***loading plots*** are now the scores and loadings plotted in the PC space.

PC space can be multidimensional, although is easily viewed in 2D space using Unscrambler, a software that caters to such Multivariate Analysis. The software contains multiple useful features that makes it easy to view, import, process and interpret multivariate data.

3 Methodology

This chapter dives into details about methods and tools used in processing of data, how data is treated for analysis, processing and description of other processed data not obtained directly from sensors, and any related parameters relevant to the processing of data

Python (Spyder) and Unscrambler X 10.3 are used for all analysis and processing of all datafiles. **Pandas**, **SciPy** and **Matplotlib** are libraries used from Python for all data analysis.

All data matrices imported in Unscrambler were in Excel(.xslx) format.

3.1 CDC Data

Cemit's Data Collector (CDC)'s IMU unit consists of a 3-axis MEMS accelerometer and a gyroscope, although just accelerometer measurements sampled in time are used for this stage of research. The CDC unit also houses a GPS, the co-ordinates for which are also used to pinpoint interesting points along the track where frequencies varied across multiple runs.

Sampling Frequency (Sr):
Accelerometer data along all three axes are sampled at a sampling frequency of 500Hz, while location data and velocity are recorded at a rate of 5Hz. Since velocity and location data were sampled at different frequencies, they could not be plotted against the same time samples.

The maximum frequency sampled by the acoustic sensors is thus 250Hz.

Subject Vehicle):

The subject vehicle is introduced in previous sections, but it is useful to denote once again that the vehicle is s freight train, notably the Skd 22, 400Hk (horsepower), described as suitable for driving in tunnel work[8].

The locomotive (including wheelset) weighs 32tonn according to the information in Grenland Rail's site, however, the locomotive is usually attached to more railway carriages transporting limestone to Norcem factory, which was not noted or obtained to the best of knowledge.

3.1.1 The S-direction

Instead of plotting acoustics data along the latitude and longitude, a referencing 's-direction' is used to quantify the distance along the track. The s-direction is used instead of calculation distance between each GPS coordinates, and is a measure of the distance from Oslo, according to information from data experts in Cemit. This standard is yet to be patented, and online sources containing proper details are not available yet, although the reference is reliably used by analyst specialists at Cemit.

Figure 3.1 shows a roughly produced reference of the distance and direction where the Brevikbanen lies in comparison to Oslo's location. The distance in kilometer, in the s-direction, is naturally expected to increase as the rail vehicle runs towards Brevik.

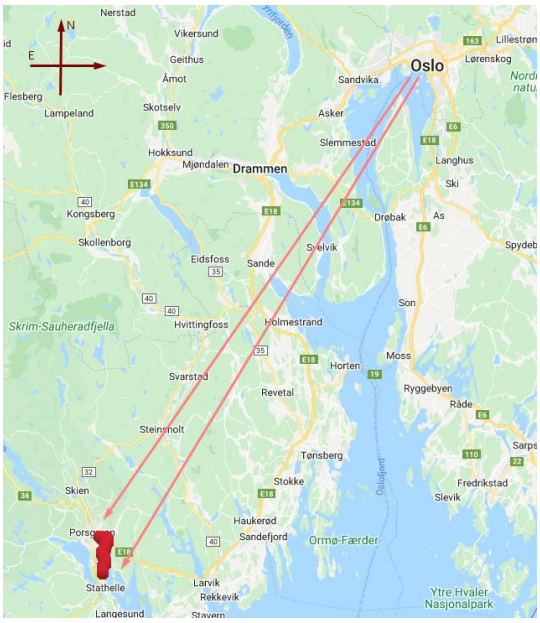

Figure 3.1 S-direction, distance from Oslo

Since GPS co-ordinates are not plotted along frequency or velocity, a reference plot showing the corresponding latitude and longitude values along the s-direction is generated specific to each dataset (although the s-data is roughly the same). Hovering over such a plot will show the GPS co-ordinates, tracing the analyzed spectra back to the original location data.

Figure 3.2 shows an example of s-direction and GPS data from one of the datasets.

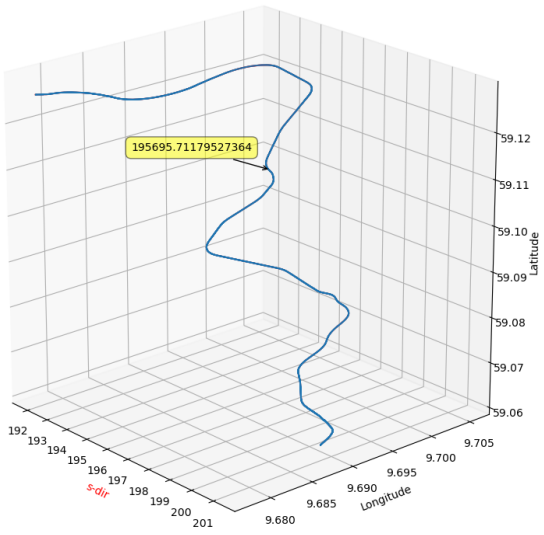

Figure 3.2 GPS plotted along s-direction

Each datafile had an accompanying datafile containing s-direction values, and had same number of datapoints as GPS data sampled at 5Hz.

3.1.2 Brevikbanen

The track along which the freight locomotive runs is a single lined track name Brevikbanen, and is currently used only in parts by freight trains for raw material transportation to Norcem's cement factory. It originally stretches approximately 11km [21] from Eidanger to Brevik, as demonstrated in Figure 3.3, however, the current usage of the track spans 9km. The track is known to have a narrow gauge of 1,067mm[21].

The experimental runs span s-directions from approximately 191.919 km to 201.276 km (distance from Oslo) where the locomotive carries limestone from limestone mine in Porsgrunn, to Norcem's cement factory in Brevik.

Experimental data were collected on runs along the track running in both directions, and therefore a 'direct' and a 'reverse' route has been marked for ease of understanding the direction along which the data is collected. The direction along which the train runs towards the Norcem factory can briefly be used to remembered as 'direct'.

As it turns out, most of the datasets used in analysis are from 'direct' runs, but data from 'opposite' runs were also analyzed, although not in similar depths.

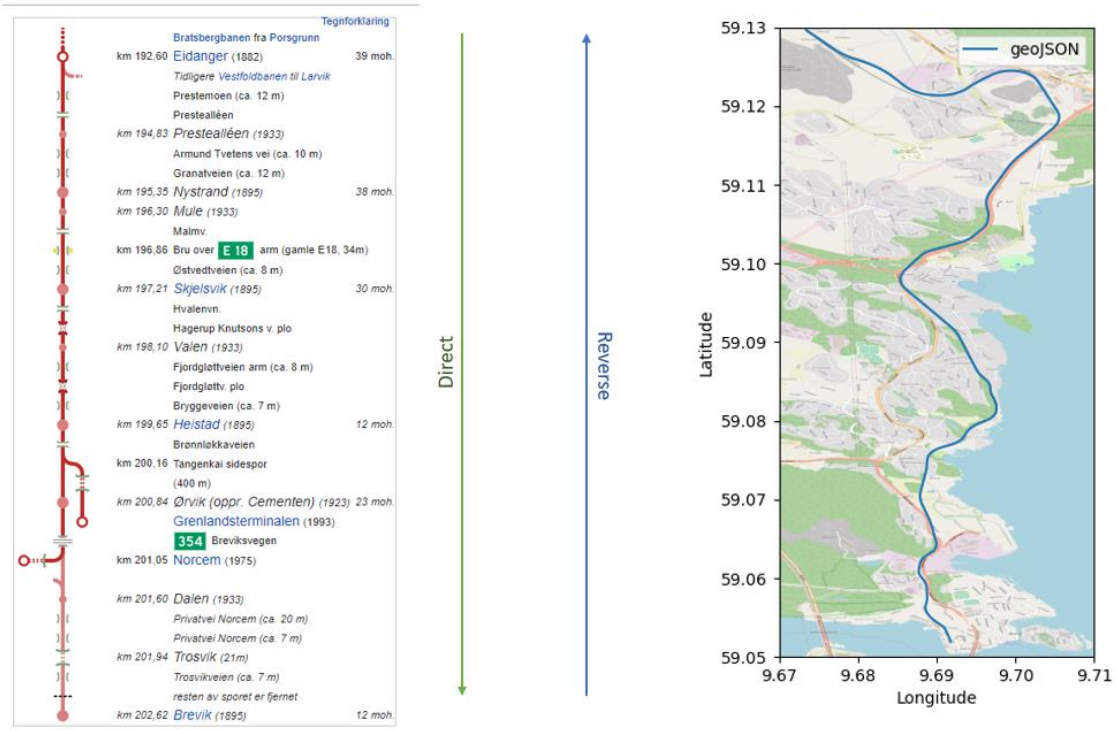

Figure 3.3 Route of Brevikbanen. Image at left shows a collected diagram of the route starting from Eidanger, ending at Brevik. Direct and Reverse directions are marked, and a map tracing the GPS coordinates of the track is shown on the right. The map on right thus shows only the track coordinates collected by CDC.

3.2 Data Treatment

The treatment of the acoustic data involves plotting time-domain data, spectrograms for all axes of each data, and plotting velocity along both time and s-directions. While spectral analysis can be run for all three orthogonal axes, the vertical direction, or z-axis, will be the

axis of scrutiny. This could be understood more well once spectrogram results from all the axes are introduced, and would lead to the understanding that the z-axis carries more relevant information related to rail-wheel dynamics.

Studying underlying relationship between frequency components from all tri-axes could even be worth a separate study. It has been found that the x and y acceleration components carry useful information at instances of track exceptions which could aid in recognizing track defects, albeit using a different time-series analysis using wavelet-based algorithm[7] - quite outside the objective and scope given the chosen methodology for analyzing time-series data, and thus it is deemed both relevant and practical to focus on just the vertical component analysis germane to this particular study.

3.2.1 Pre-analysis of relevant data

A total of 23 datafiles were used for spectral analysis, amongst which 17 files were from 'direct' runs, and 6 were from 'indirect' runs. Although more datasets were available, no more were included since it would start to take longer for processing spectrograms. A separate python was created (datafiles.py) for storing these excel file names were used to make usage of analysis codes easier and more robust. The file can be found in GitHub as datafiles.py

Most of the analysis were done using datafiles from 'direct' routes. Whether a datafile was from direct or reverse route was understood by plotting s-direction against time. Figure 3.4 shows 2 such plots that would show information about the direction of the locomotive's route.

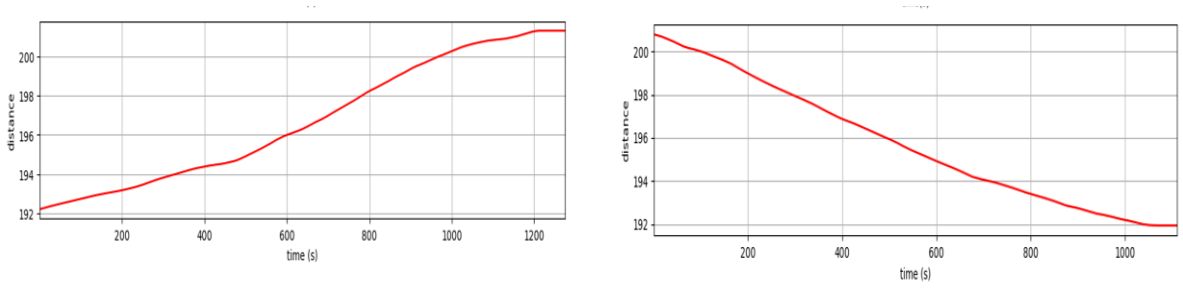

Figure 3.4 (Left) s-direction vs time plot, showing the locomotive's run from Porsgrunn to Brevik (Right) reverse direction from approx. 201 km to 190 km, from Brevik to Porsgrunn

Since many operations were repeated throughout several code files, the following codes were developed as functions, and later imported as needed into code files that ran spectral analysis. All codes are available in the mentioned names in GitHub (Appendix B).

- `load_from_df.py`: contains 2 functions, first of which takes in file number and returns the datafram from that excel file, while the second takes in the dataframe as argument and retuns vectors for time stamps and the 3 axes signals

- `spectra_signals.py`: contains functions that takes in accelerometer data as arguments and generates spectrogram data. The functions return the frequency segments, segmented times and amplitudes calculated for the FFTs

- `visuals.py`: contains various functions for plotting spectras across various codes, and exporting FFTs and spectrogram data as excels.

- `spectraAnalysisFunctions.py`:tcontains function for calculating standard deviation spectra, and functions that calculate minimum length between all files, a necessary adjustment made because not all datafiles have sample number of samples, and generates unequal FFTs, which would become an issue when calculating averaged spectra.

3.2.2 Spectrograms

Spectrograms, as seen earlier, are essentially stacked FFTs, shown usually in a 2D colormapped plot along frequency vs time axes. The following parameters are provided to the spectrogram function [18] in Python :

- *nperseg*, time window: 610 samples (equal to 1.22s)
- *window*, windowing function : 'blackman'
- *noverlap*, number of overlapping samples : 100 samples (equal to 0.2s)
- *fs*, sampling rate : 500

Resultant spectrograms have dimensions that depend on the number of data samples in a datafile. For the first datafile from 'direct' datafiles, for example, a total of 653,133 samples sampled from 500 Hz, would mean the duration of that run is

*Number of samples * sampling period = 653,331 * 0.002 = 1306.266s*

Performing FFT on each window of 610 samples, where 100 samples are overlapped, would mean 510 samples are stored for an FFT. If a window has 510 samples, the duration of a window is then,

*Number of samples (time window) * sampling period = 510 * 0.002 = 1.02s*

The total number of time segments is then 1306.22/1.02 = 1208, for spectrogram generated from this file. This is also the total number of FFTs from this datafile, each FFT being plotted along the time segments

The total number of frequency bins, utilizes time duration of 1.22s, and hence the Fr equals

Fr = 1/1.22s = 0.819Hz , using Equation 1.8

The number of frequency bins is then 250Hz/0.819Hz $\approx$ 306 bins.

The number of time segments vary for each file according to the number of samples, but the time and frequency resolution are constant, since time resolution and frequency resolution are dependent on the time window sample and sampling rate, which are same for all files.

3.2.3 Time Axes for Spectra and Other Time-Series Data

As seen from calculations, the duration for which FFTs are generated from the spectrogram is 1.02s. When spectrogram is plotted along time axis, therefore, a datafile where the total

duration of the experimental run is 1306s, for example, will have approximately 1280s (1306*1.02) in its spectrogram duration.

When comparing timing along x-axis between velocity and spectrogram, this feature is exploited. Of course, this is perhaps not the best approach, since time resolution is not always the same, however, the benefit of having almost identical time axis for both spectrograms and velocity plots proved to be useful.

3.2.4 Comparing spectra and time-series data

The spectral data alone should expose patterns and variation in signal strength of different frequencies for a particular run. Dominant frequencies on each axis, for example, could be found from just observing the spectra. The goal, however, is to understand and diagnose the acoustic 'soundscapes' in real time, and that demands understanding the acoustics of the rail-wheel interactions in terms of more than just the common, dominant frequencies.

And as such, the spectrograms will be analyzed along the velocity of the rolling stock, in attempts to see if velocity bears a change in the spectrum along time axis, and on the intensity of the signal.

Aforementioned plotting of s-direction along the GPS coordinates, as shown in Figure 3.2, should help in tracing the location in latitude and longitude, given s-direction value is known.

The flow of analysis is therefore-

- To generate spectrograms for a dataset/run
- To plot velocity along time and s-direction, plotted in same figure as subplots for comparison
- To have a referencing s-direction and GPS plot, to be able to pinpoint an exact location along a track to see where acoustic of interest lay.

Figure 3.5 shows a demonstration of such a flow using data from file ***20200824T1135***. It is also useful to denote that the file numbers are included in all analysis, along with the axis for which spectrum is generated.

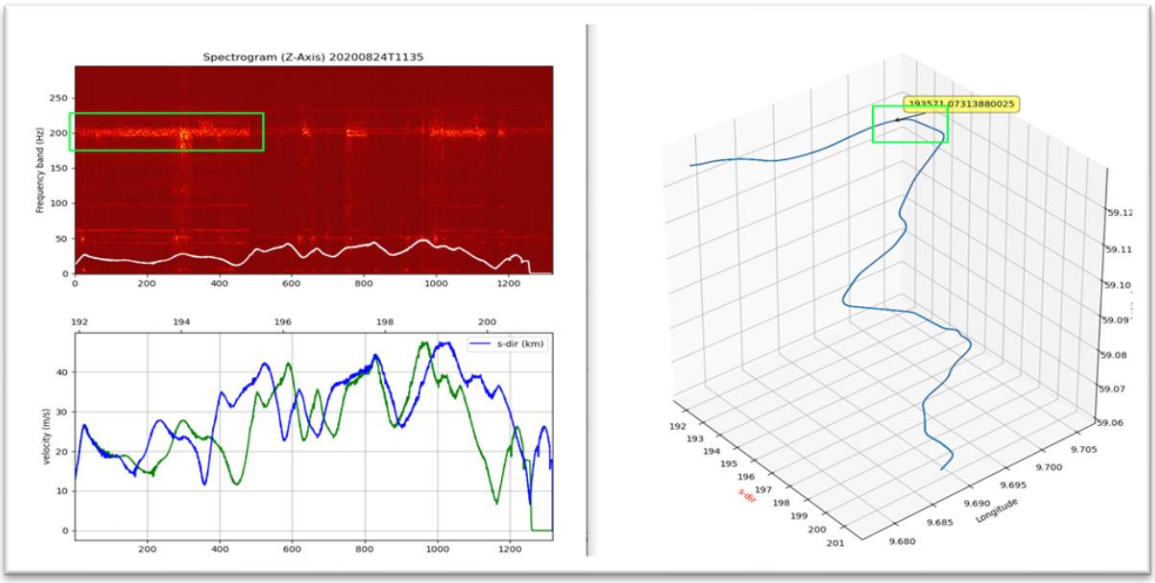

Figure 3.5 Using spectrogram, velocity plot and s-data plot to draw observations

In the plots in Figure 3.5, a few details owe explanation before results can be drawn for more datasets. The velocity plot, right beneath the spectrogram, is plotted from the s-data file generated for each original dataset. Generation of this s-data file is done by data specialist Wathsala Upamali at Cemit.

Time and s-direction data from these files are used along x-axes since the velocity is the same regardless. However, the s-data can 'stretch' a little back and forth since each unit in kilometer in s-direction does not necessarily equal to each unit in time axes. Nevertheless, the two x-axes were plotted to use time as reference from the spectrogram plot, and to use that time stamp to find the s-direction value from the velocity plots (exact value found out using yellow markers that show up on hover). The s-direction value can then be used to trace the latitude and longitude co-ordinates (using 3D plot on right of Figure 3.5))

Figure 3.6 shows another demonstration, for clarity.

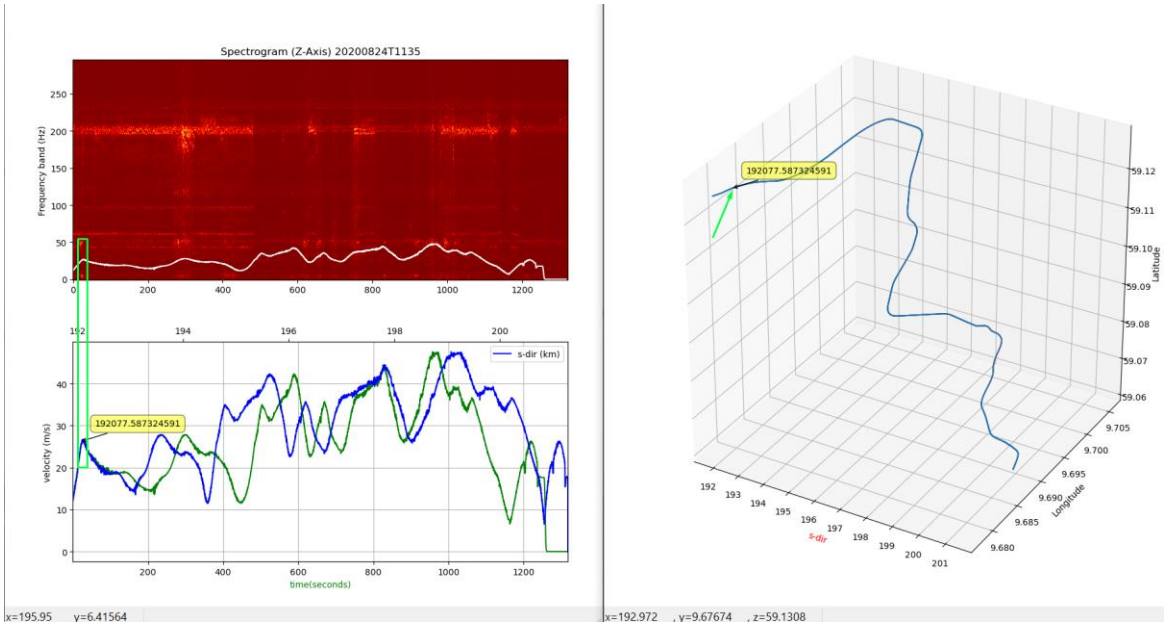

Figure 3.6 S-direction data traced from velocity plots and spectrum

Although somewhat lengthy, the plots help provide an overview of how velocity varies along distance and the spectrogram at the same time. The white line plotted on top of the spectrogram is also the velocity plot line along time axis, but is quite obviously not scaled to a height that would be suitable for a better view. It is left on the spectrogram anyways, yet as an attempt to have as much information as possible within few plots. The line is, of course, not accurate since a separate axis for velocity along y-axis is not given, and can simply be dropped off or disregarded in case it causes more confusion for anyone running the codes without a heads-up on this.

3.3 Spectral Processing for Specific Analysis

While techniques mentioned this far can be used to analyze individual datasets to a reasonable degree, it can become hectic and rather time-consuming to have to look into individual datasets when files become more in number. In order to be able to make overall observations and comparisons, a reference spectrum can be designed from **linear averaging** of multiple spectra

into one. This referencing spectrum representing most of the dominant frequencies, could help in a number of ways, including:

- Reducing the effect of noisy signal: much like averaging of signals in time-domain, taking an averaged spectra can highlight frequencies that are present among along most runs, adding to the amplitudes, and will cancel out signals that are random.

- Having a preliminary reference: At the absence of reference 'acoustic signatures' that would have to be generated to performed advanced multivariate analysis such as classification using PCA or regression using PLS-R, an averaged spectra could be analyzed to have a preliminary understanding of the main frequency components for the given track and vehicle.

- Comparing with a **standard deviation spectrum**: With an averaged spectra as reference, the variation of datasets compared to this reference can be used to identify special areas for further analysis

And so, Python codes for generating a mean spectra and corresponding standard deviation spectra, possible as plots for each frequency spectrum, are also included in GitHub names as *spectra_average.py*

Elimination of certain frequencies:

It must be notified at this stage, that the first few frequencies, especially from 0 Hz to 5Hz, are not taken into consideration when generating spectrograms, 3D spectras, or PCA analysis. This is because the power presernt in these frequency components are many folds higher than the rest of the frquencies, making their visibliites extremely low along the rest of the spectrogram. An exhibit of this is shown in Appendix C. The top image in the appendix shows a spectrogram with all frequencies taken into account, while the bottom image shows the same spectrogram without the frequencies. The frequencies are, of course, not deleted from any files or stored variables, just not selected when generating spectra or performing PCA.

3.4 Principle Component Analysis

PCA is known to reduce-dimensionality, i.e, reducing the number of variables by utilizing only the most important ones in form of Principle Components, which is the new, most effective variable are expressed as a linear set of co-efficients. The largest variance amongst the samples is explained with these PCs, and can be a powerful tool to use for feature extraction. With this understanding, PCA is performed on the averaged spectra of z-axis, the outcome of which should indicate the most prominent Principle Components, in the form of a spectra.

3.4.1 Disclaimers Regarding PCA on Spectral (FFT) Data

While PCA is popularly used to understand and observe trends in data, to identify clusters, outliers, and in classification problems[22], applying PCA to serially timed FFTs is not a method known to have been applied often.

In fact, PCA has been applied before to assist in reducing the number of FFT co-efficients[22] (signal values in frequency domain), in order to facilitate storage of data, for example. In another instance, it has even been used in rather comparison with FFT in effectively identifying heart rate and respiration rate, according to a 2015 conference journal published in Sweden[23].

Moreover, PCA has been shown to be effective when applied to spectroscopic measurements such as NIR spectroscopy, where number of wavelengths are reduced with the help of PCA[24]. The spectral data for this case for instance, was not FFT, more notably, not spectra that are taken of a time-varying process, as is the one attempted in this study.

Therefore, PCA done on the FFT data as part of study of this thesis, where the FFTs are not only taken along the time-axis but also used as the data samples for PCA, is quite unconventional, and hence are expected to yield results that could have different interpretation than how it is usually done.

Suggestions to improve and explore more effective ways to perform PCA using spectral FFTs are discussed more into in later chapters. However, performing this initial PCA on the averaged z-axis spectra should, in the least, expose frequencies that are not common throughout this representative spectrum, and the first PC, essentially an acoustic spectrum that contains frequencies accounting for the largest variation for the averaged 'run' spectra, could be registered as a 'latent phenomenon', the frequency composition of which could be worth analyzing.

3.4.2 X-Variables and Objects

The spectrogram is adjusted for proper labels and orientation, and then exported from Python to be imported into Unscrambler as excel data.

The X-variables are the sampled frequencies, and are same as the number of frequency bins calculated in Section 3.2.2, and the number of objects, similarly, is equal to the number of time segments, or the number of FFTs. Figure 3.7shows what the data matrix looks like after it is imported in Unscrambler.

Z_axis_avg_		6.557377049	7.377049180	8.196721311	9.016393442	9.836065573	10.65573770	11.47540983	12.29508196	13.11475409	13.93442622	14.75409836	15.57377049	16.39344262	17.21311475	18
		1	2	3	4	5	6	7	8	9	10	11	12	13	14	
0.61	1	0.0004	0.0004	0.0005	0.0005	0.0006	0.0009	0.0007	0.0010	0.0012	0.0005	0.0004	0.0005	0.0006	0.0004	
1.63	2	0.0006	0.0005	0.0006	0.0007	0.0007	0.0005	0.0005	0.0009	0.0012	0.0009	0.0007	0.0004	0.0004	0.0005	
2.65	3	0.0003	0.0003	0.0005	0.0006	0.0007	0.0005	0.0004	0.0006	0.0010	0.0008	0.0005	0.0003	0.0003	0.0004	
3.67	4	0.0003	0.0004	0.0005	0.0004	0.0004	0.0005	0.0005	0.0010	0.0012	0.0010	0.0005	0.0004	0.0005	0.0003	
4.69	5	0.0006	0.0006	0.0005	0.0005	0.0009	0.0010	0.0010	0.0008	0.0006	0.0005	0.0005	0.0003	0.0005	0.0006	
5.71	6	0.0005	0.0004	0.0003	0.0005	0.0008	0.0009	0.0011	0.0016	0.0017	0.0014	0.0011	0.0009	0.0007	0.0004	
6.73	7	0.0004	0.0004	0.0003	0.0005	0.0006	0.0006	0.0010	0.0013	0.0008	0.0007	0.0007	0.0005	0.0004	0.0005	
7.75	8	0.0010	0.0008	0.0006	0.0005	0.0009	0.0012	0.0015	0.0016	0.0012	0.0006	0.0005	0.0005	0.0005	0.0005	
8.77	9	0.0008	0.0008	0.0009	0.0009	0.0006	0.0005	0.0012	0.0017	0.0021	0.0018	0.0009	0.0005	0.0004	0.0005	
9.79	10	0.0021	0.0015	0.0017	0.0015	0.0010	0.0009	0.0016	0.0023	0.0019	0.0013	0.0011	0.0008	0.0008	0.0008	
10.81	11	0.0019	0.0014	0.0010	0.0009	0.0014	0.0016	0.0010	0.0015	0.0014	0.0009	0.0006	0.0005	0.0004	0.0004	
11.83	12	0.0009	0.0006	0.0005	0.0005	0.0009	0.0012	0.0015	0.0017	0.0016	0.0015	0.0012	0.0009	0.0004	0.0003	
12.85	13	0.0005	0.0004	0.0004	0.0006	0.0009	0.0012	0.0014	0.0011	0.0014	0.0016	0.0012	0.0006	0.0007	0.0006	
13.87	14	0.0005	0.0006	0.0006	0.0005	0.0004	0.0006	0.0012	0.0014	0.0016	0.0016	0.0011	0.0009	0.0005	0.0004	
14.89	15	0.0004	0.0004	0.0003	0.0004	0.0004	0.0004	0.0009	0.0014	0.0011	0.0015	0.0013	0.0009	0.0007	0.0005	
15.91	16	0.0006	0.0005	0.0006	0.0007	0.0007	0.0009	0.0015	0.0023	0.0015	0.0013	0.0014	0.0007	0.0008	0.0005	
16.93	17	0.0004	0.0005	0.0006	0.0003	0.0005	0.0011	0.0012	0.0018	0.0015	0.0009	0.0018	0.0020	0.0010	0.0005	
17.95	18	0.0004	0.0003	0.0004	0.0004	0.0004	0.0014	0.0014	0.0022	0.0038	0.0022	0.0017	0.0016	0.0005	0.0004	
18.97	19	0.0003	0.0003	0.0004	0.0006	0.0006	0.0012	0.0014	0.0017	0.0033	0.0023	0.0011	0.0014	0.0010	0.0004	
19.99	20	0.0003	0.0002	0.0004	0.0006	0.0005	0.0006	0.0014	0.0013	0.0021	0.0025	0.0010	0.0006	0.0006	0.0003	
21.01	21	0.0003	0.0004	0.0004	0.0006	0.0004	0.0009	0.0022	0.0019	0.0017	0.0018	0.0008	0.0007	0.0010	0.0008	
22.03	22	0.0002	0.0003	0.0003	0.0007	0.0011	0.0012	0.0030	0.0033	0.0015	0.0017	0.0019	0.0011	0.0009	0.0013	
23.05	23	0.0007	0.0006	0.0004	0.0004	0.0007	0.0008	0.0015	0.0046	0.0037	0.0016	0.0012	0.0006	0.0005	0.0004	
24.07	24	0.0005	0.0004	0.0008	0.0011	0.0012	0.0014	0.0033	0.0051	0.0043	0.0016	0.0009	0.0007	0.0007	0.0011	
25.09	25	0.0022	0.0018	0.0013	0.0017	0.0031	0.0049	0.0101	0.0151	0.0125	0.0053	0.0020	0.0008	0.0007	0.0006	
26.11	26	0.0014	0.0012	0.0012	0.0023	0.0041	0.0051	0.0089	0.0131	0.0091	0.0035	0.0021	0.0016	0.0010	0.0013	
27.13	27	0.0026	0.0021	0.0023	0.0020	0.0044	0.0082	0.0089	0.0118	0.0091	0.0039	0.0028	0.0021	0.0015	0.0011	
28.15	28	0.0023	0.0026	0.0037	0.0040	0.0046	0.0058	0.0052	0.0056	0.0056	0.0024	0.0020	0.0018	0.0015	0.0011	
29.17	29	0.0014	0.0017	0.0019	0.0025	0.0043	0.0056	0.0064	0.0062	0.0049	0.0021	0.0012	0.0016	0.0012	0.0005	
30.19	30	0.0017	0.0022	0.0020	0.0026	0.0027	0.0021	0.0020	0.0014	0.0023	0.0019	0.0011	0.0006	0.0006	0.0004	
31.21	31	0.0007	0.0008	0.0010	0.0015	0.0017	0.0011	0.0013	0.0016	0.0018	0.0016	0.0012	0.0006	0.0004	0.0003	
32.23	32	0.0006	0.0004	0.0004	0.0006	0.0009	0.0007	0.0007	0.0010	0.0011	0.0011	0.0008	0.0004	0.0004	0.0005	
33.25	33	0.0005	0.0006	0.0007	0.0006	0.0006	0.0008	0.0012	0.0011	0.0006	0.0007	0.0006	0.0005	0.0005	0.0004	
34.27	34	0.0003	0.0003	0.0003	0.0006	0.0009	0.0006	0.0010	0.0014	0.0008	0.0006	0.0007	0.0004	0.0004	0.0003	
35.29	35	0.0005	0.0004	0.0007	0.0007	0.0006	0.0007	0.0010	0.0013	0.0009	0.0009	0.0008	0.0004	0.0003	0.0003	

Figure 3.7 Loaded X data-matrix into Unscrambler X. The samples, or FFTs, are the objects, while the frequencies (bins) are the variables

The data matrix only contains amplitude values, hence is not processed for scaling. The data is, however, mean centered. Since the analysis is initial, PCA is set to show 12 PCs, assuming that the data is noisy, and important PCs can still be present in higher components.

4 Findings and Results

This section presents results from spectrograms of individual datafiles (runs), of averaged and deviation spectra, and results from PCA done on reference (averaged) spectra. The subsections show the relevant results, and reports on observations based on them.

File numbers mentioned here correspond to the index used to read the files into the program. Since 17 files were analyzed, index 0-16 is used. The file names have information on then, such as date and time, which is why filenames were preserved too. The file names can be seen displayed on the title of relevant plots.

4.1 Spectral Methods

4.1.1 Time-domain data and Velocity

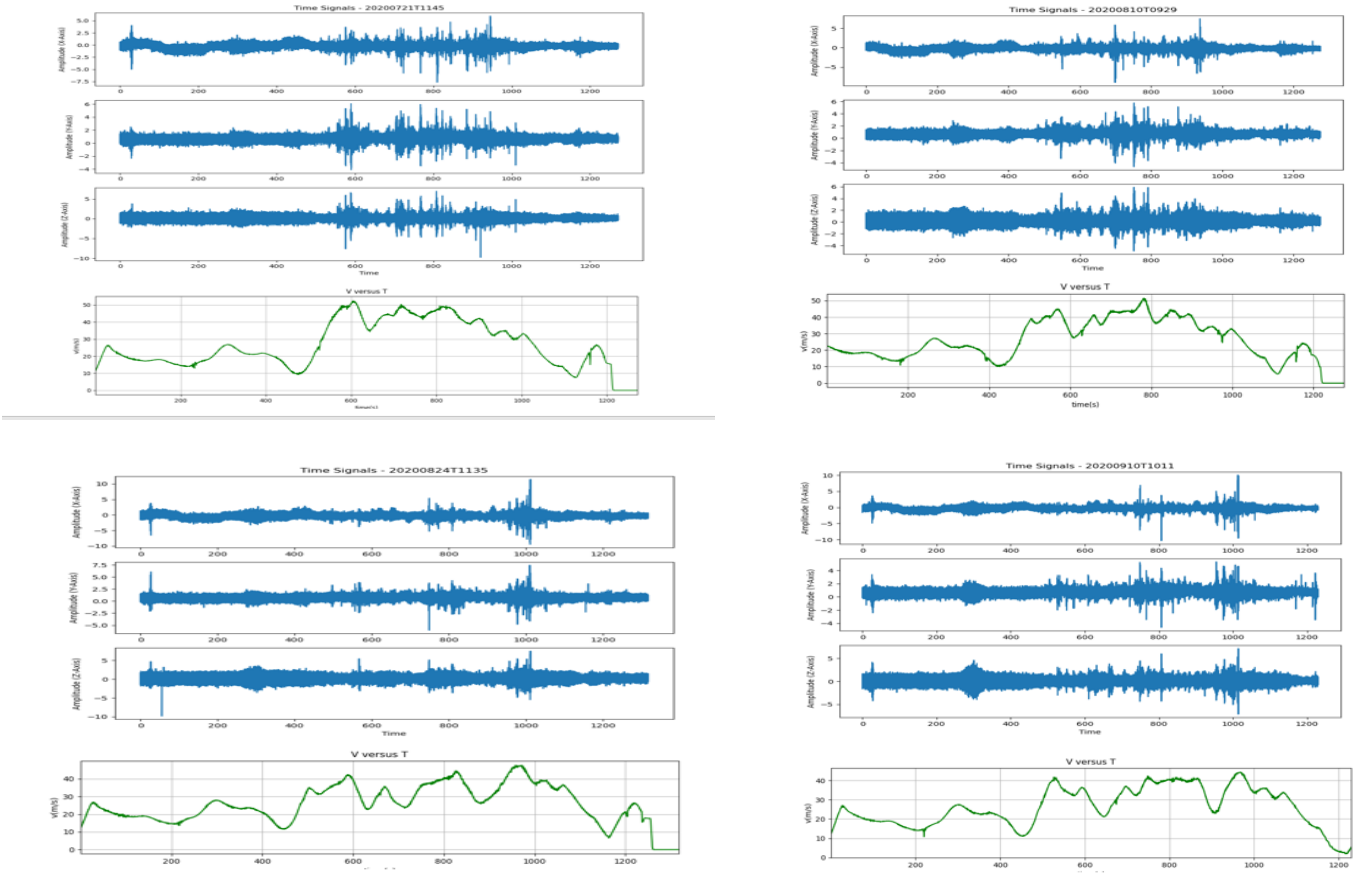

Figure 4.1 Time signals from 4 of the 17 datafiles (file 0[top left], 5[top right], 10[bottom left], 15[bottom right]), all from direct routes. The velocity changes up to 500s appears to be almost identical, and the time signals reflect the same.

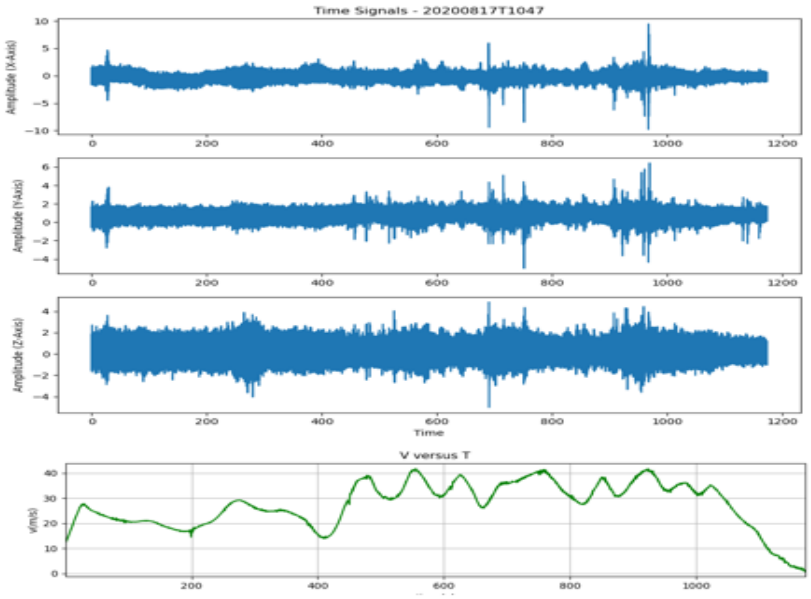

Figure 4.2 File 8, with distinguishable variation in acceleration compared to most dataset from 'direct' runs.

Observations:

- Unlike all the other runs, file 15 does not have a sharp rise in velocity at the beginning of the run, and is telling from the time domain signal where a spike is missing, which is existent on all other runs shown in Figure 4.1and Figure 4.2

- Velocity changes at the end of the run are very similar, if not identical, for file 0, 5 and 10. This can also be observed on time-domain signal where the signal appears to be pinched out at the timestamp where there is a drop in velocity at 30km/h. This fall to 30km/h and an instant rise of velocity is missing in files 15 and 8, and does not appear to have a pinched pattern at the end of the run.

- Runs 0 and 5 appear to have higher amplitudes in time domain signal, and are the only runs where velocity reaches close to 5km/h.

4.1.2 Spectrograms – X,Y,Z Axis

Spectrogram results from the first datafile is demonstrated for initial observation of tri-axis spectra. Not all of the 17 files are shown, but 4 of them are chosen to show commonalities. Indirect route data are not observed or analyzed, given the scope and limitation of time.

Spectrogram from 0th, X, Y, Z axis:

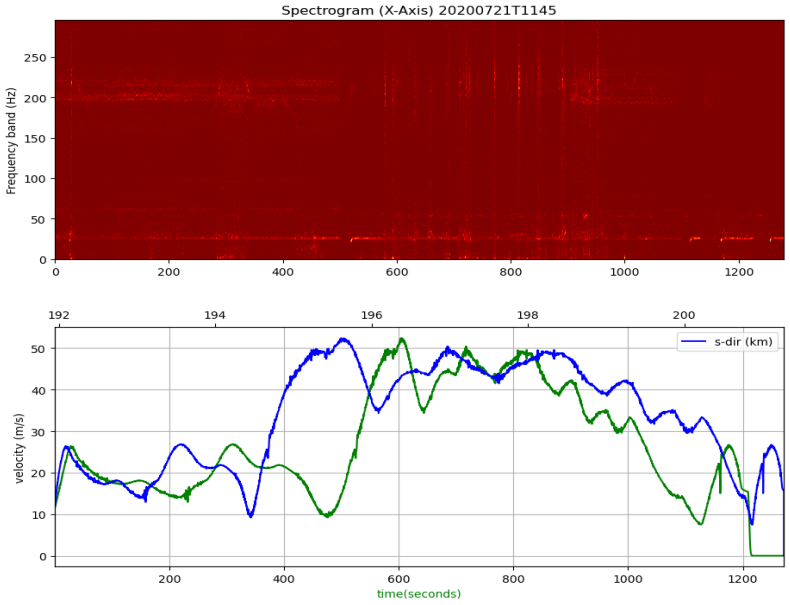

Figure 4.3 Spectrum X-Axis, 0th file, direct route

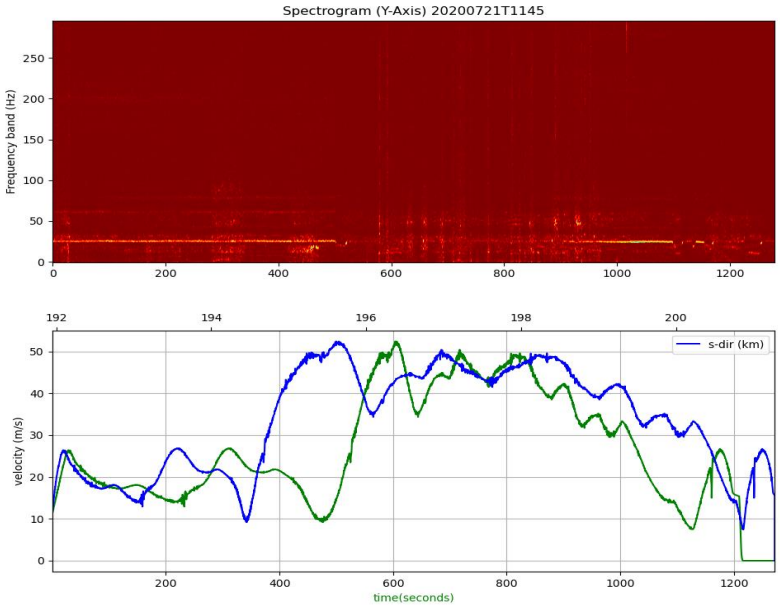

Figure 4.4 Spectrum Y-Axis, 0th file, direct route

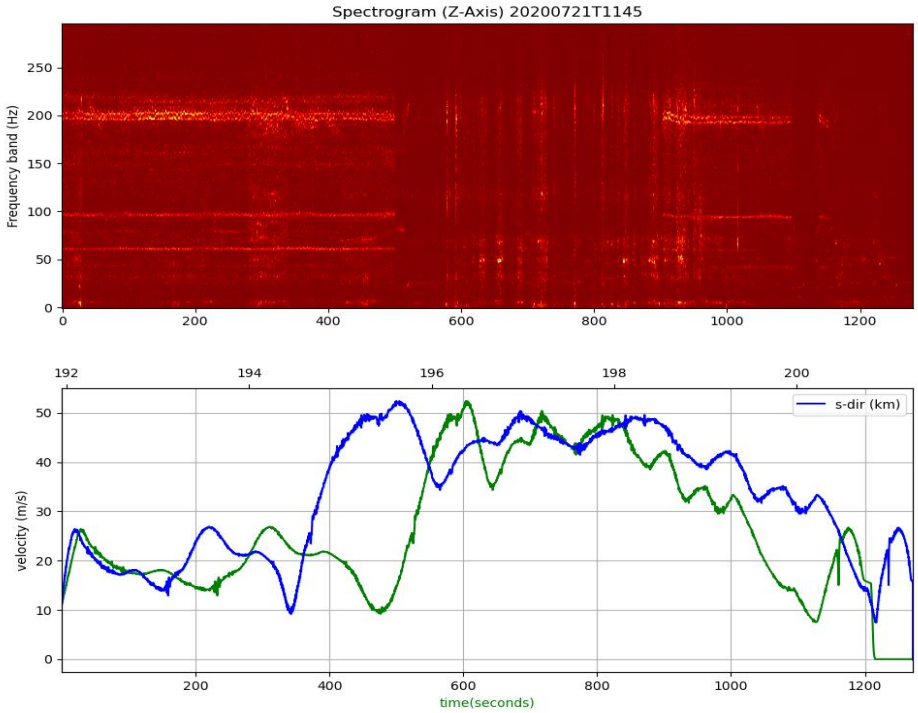

Figure 4.5 Spectrum Z-Axis, 0th file, direct route

Observations from Figures 4.3, 4.4, 4.5:

- Time stamps in spectrograms where the locomotive appears to accelerate seem to create vertical streaks along the frequency axis, visible along the start *t = 15s, 250s < t < 280s, 500s < t < 950s* (approx.), true across all axes

- Constant frequencies, or hereafter referred to as '***dominant frequencies'***, visible along **25Hz**, **60Hz**, and in ranges from **198Hz** to **220Hz** in x-axis.

- A dominant frequency of **25Hz** appears distinctive in the y-axis spectrum.

- Looking at z-axis spectra, it can be summarized that it displays most of the dominant frequencies as in x and y spectra, with the exception of the lower **25Hz**. The distinction in the longitudinal streaks along frequency axis from *t = 500s* to *t = 1000s* is the most visible along this direction.

- It might be helpful to note that the vehicle, for his run, reached a maximum velocity of **52km/h**

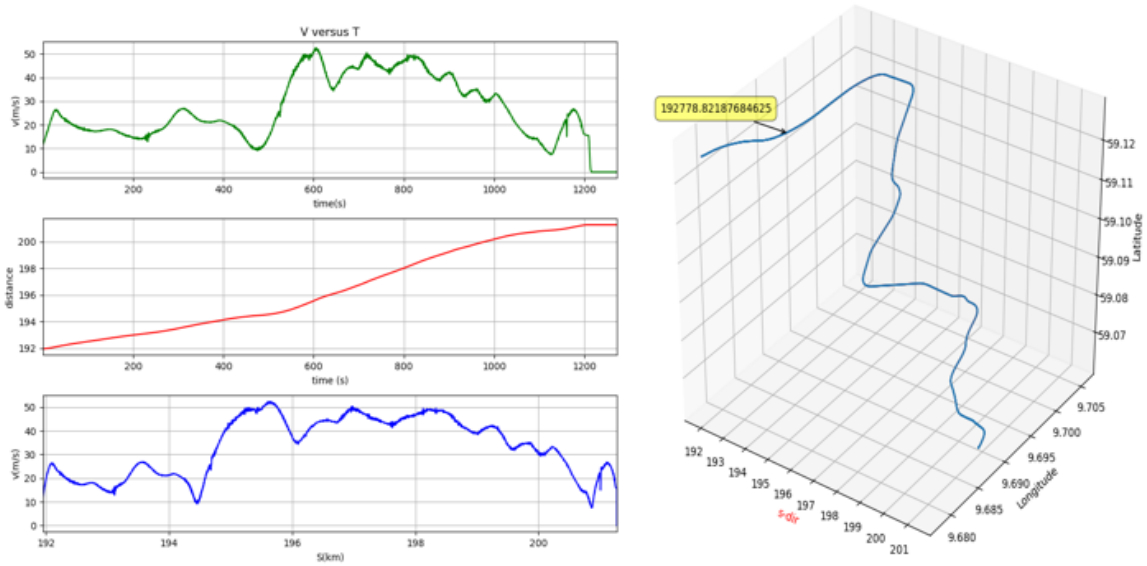

Figure 4.6 S-data and velocity plots to confirm the direction (direct/reverse)

An additional analytical code is written, that plots analytical data of every s-data file, which contains velocity and GPS coordinates, all in same sampling frequency of 5Hz. Figure 4.6 shows the complementary plots for the 0th file, along with the referencing s-direction 3D lot with GPS coordinates.

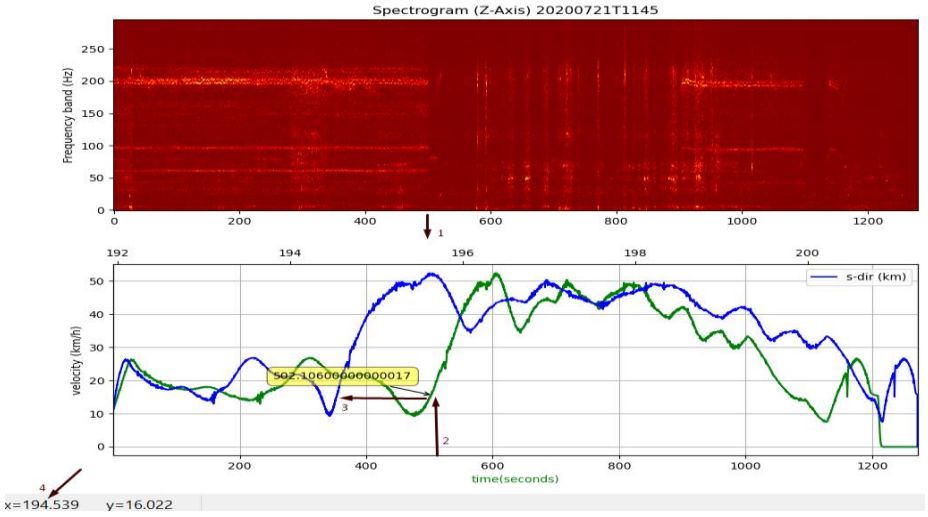

Figure 4.7 Tracing s-direction value for vertical streaks from t = 500s, using spectrogram and velocity plots, 0th file

Figure 4.7 demonstrates how values are read using the two graphs, and used in the 3D plot to track the GPS coordinates, exhibited in Figure 4.8. The portion of this s-value is also shown in the original Google Map which shows the track coordinates along a real map, Figure 4.9. This map, with the GPS coordinates plotted using *geoJSON* file, is also using codes obtained from data specialists at Cemit.

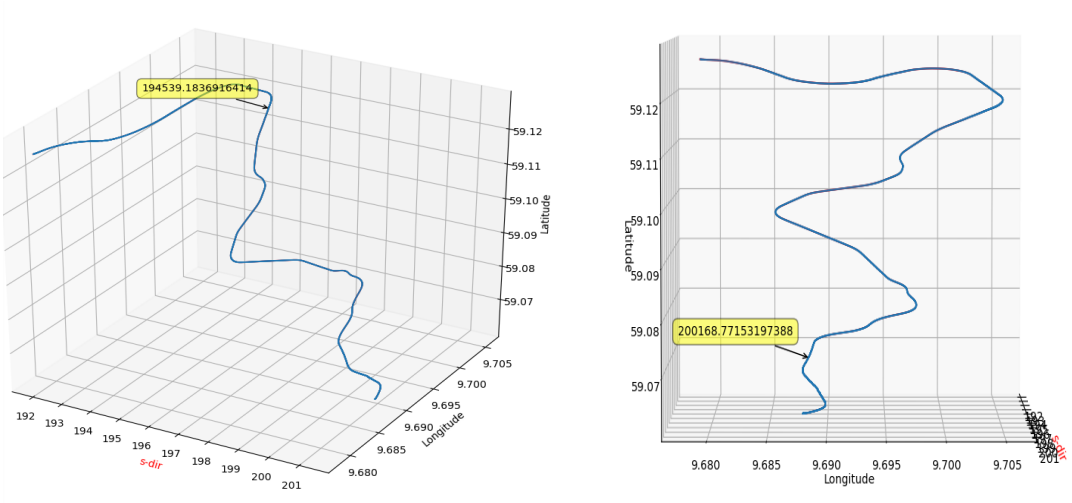

Figure 4.8 Tracing GPS coordinates using s-direction marker
in the refencing 3D plot

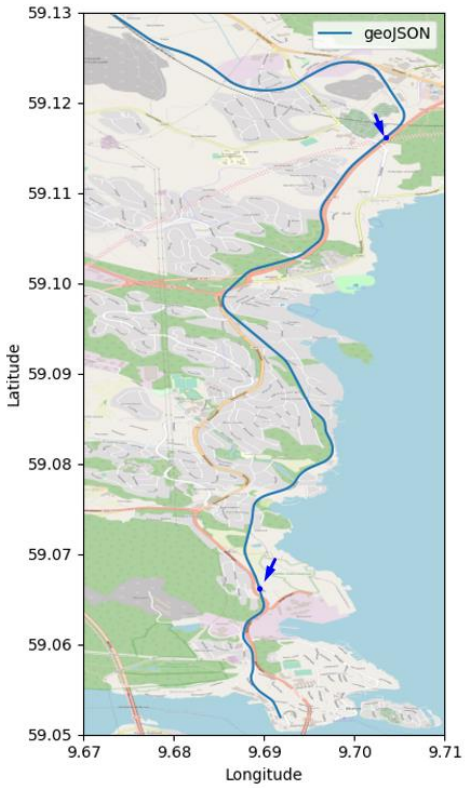

Figure 4.9 Part of original track along which experiment was conducted. The blue arrows show the section of track where the intense longitudinal streaks show up in z-axis spectrum

Spectrogram of X-Axis from 2nd , 5th , 10th and 15th datafiles:

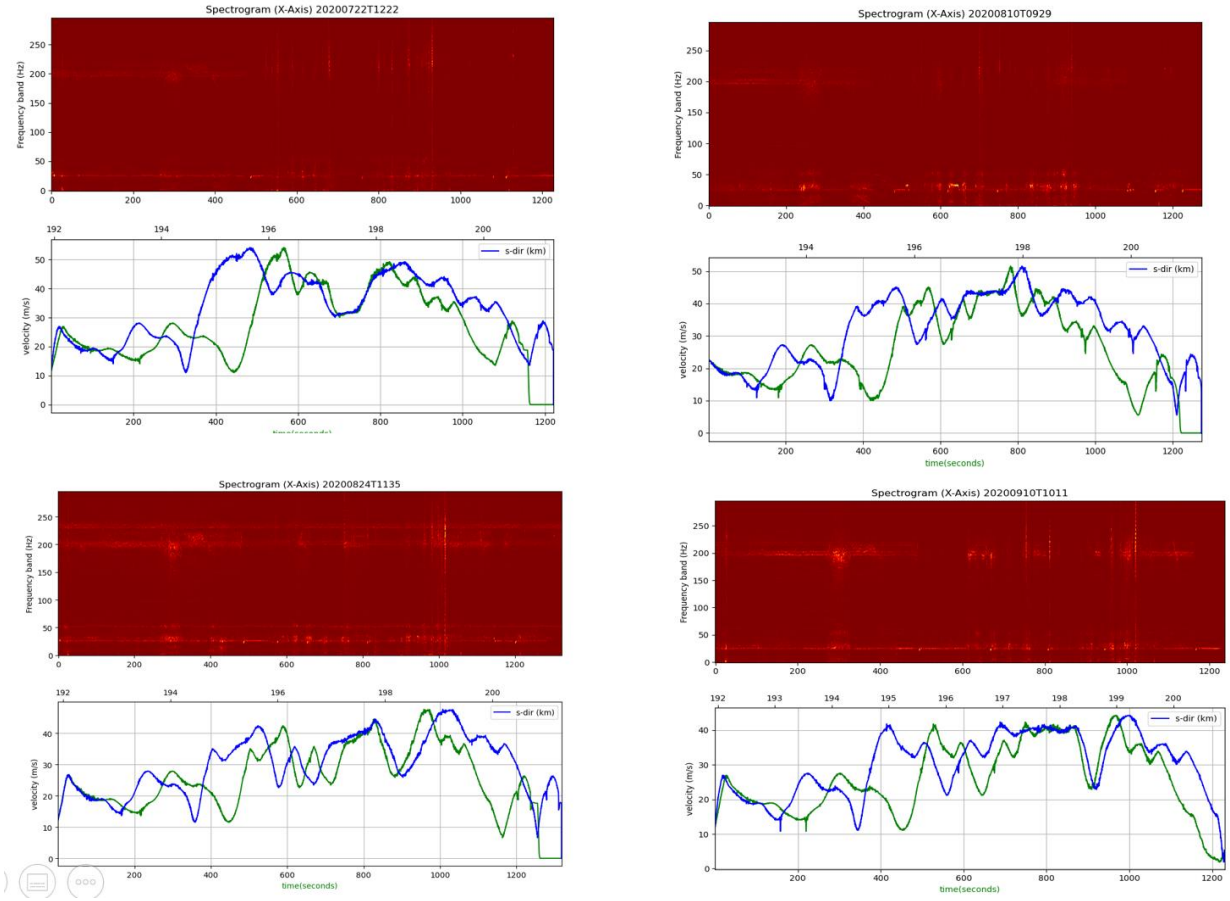

Figure 4.10 Spectrograms of x-axis (longitudinal acceleration) from 4 of the 17 files analyzed. The first 8 digits of file number contains date the data is collected on. Acceleration of the locomotive is very similar at for first 400s. Longitudinal streaks visible between times 500s to 1000s approximately, common amongst all spectra.

The streaks previously observable in x-axis of 0th file is also observable in more files from 'direct' route, as shown in Figure 4.10. File 10, bottom left of the figure, shows much more visible frequencies in the higher band (150Hz to 250Hz) than the other runs.

Spectrogram of Y-Axis from 2nd , 5th , 10th and 15th datafiles:

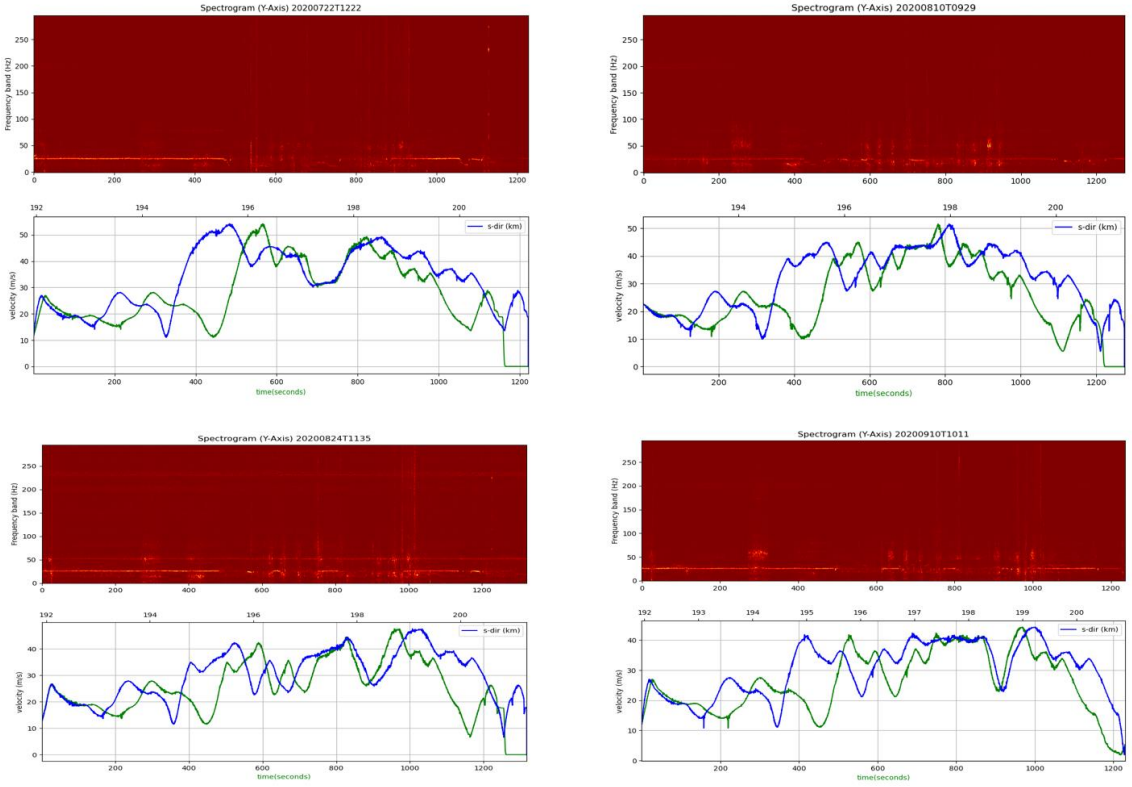

Figure 4.11 Spectrograms from 4 of the 17 'direct route' datafiles from y-axis (lateral acceleration). Very distinct, repeating patterns can be observed on lower band of frequency [10Hz – 30Hz approximately], with a spot seen occurring at 300s on all runs.

Figure 4.11 contains spectra of same files as Figure 4.10 for the lateral y-axis. Dominating frequencies along this axis appear to be more in the lower ranges (10Hz - 50Hz), with once again, more pronounces and even fairly visible frequencies exhibited by file 10, bottom left of figure.

Spectrogram of Z-Axis from 2nd , 5th , 10th and 15th datafile:

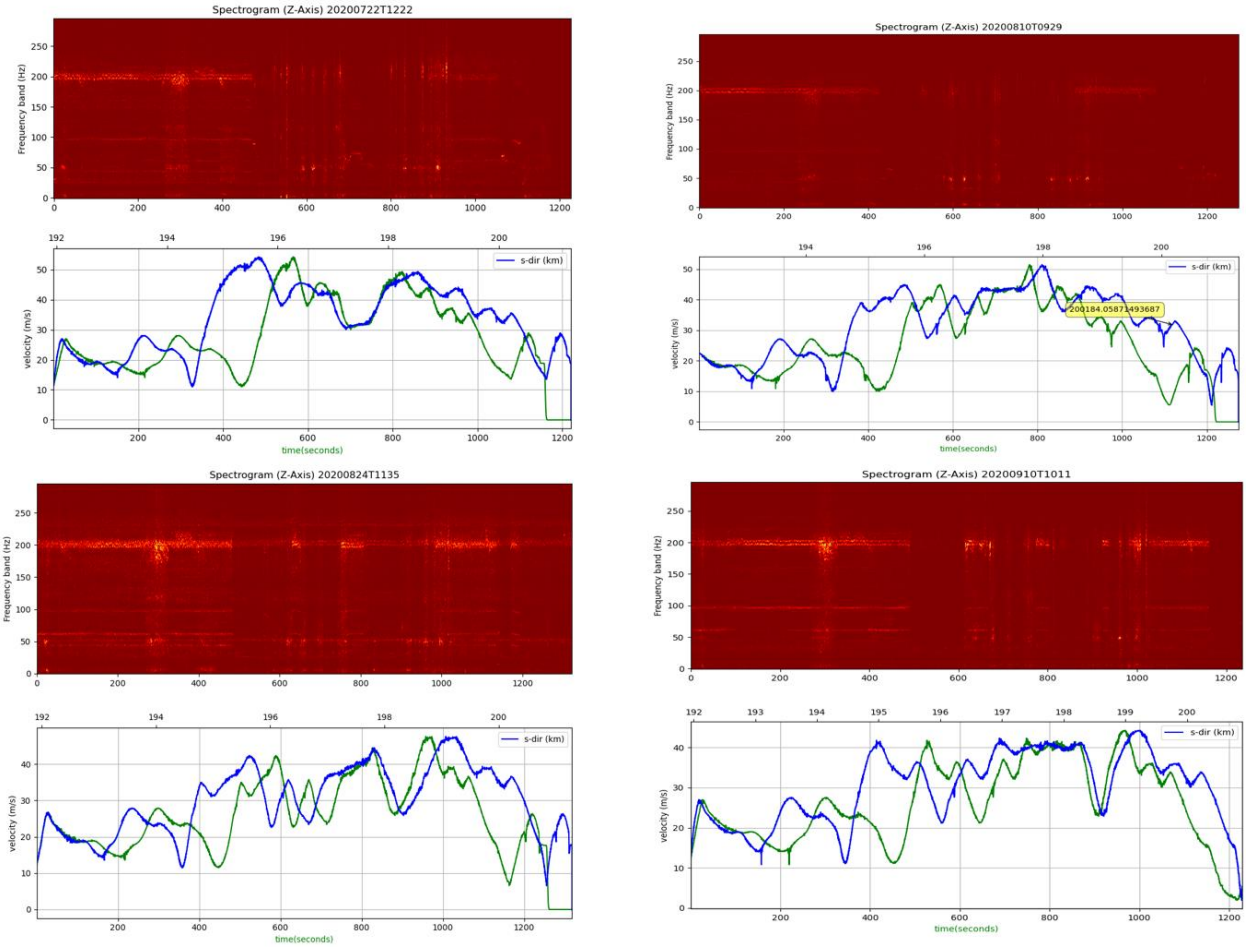

Figure 4.12 The vertical acceleration in spectrogram. An underlying pattern can be identified, but the strength of signals at some of the bands of frequencies seen to vary a lot in intensity.

Figure 4.12 shows perhaps the most detailing spectra of all direction, the z-axis spectra for the same previous runs. This axis clearly vibrates at frequencies across multiple ranges, noticeably in frequencies greater than 50Hz, at 100Hz and around 200Hz, which are similar to what was observed for z-axis for 0th file, too. The pattern that can be schemed from a glance at z-axis spectra were quite constant across all direct files, apart from a few exceptions, two of which are shown in Figure 4.13.

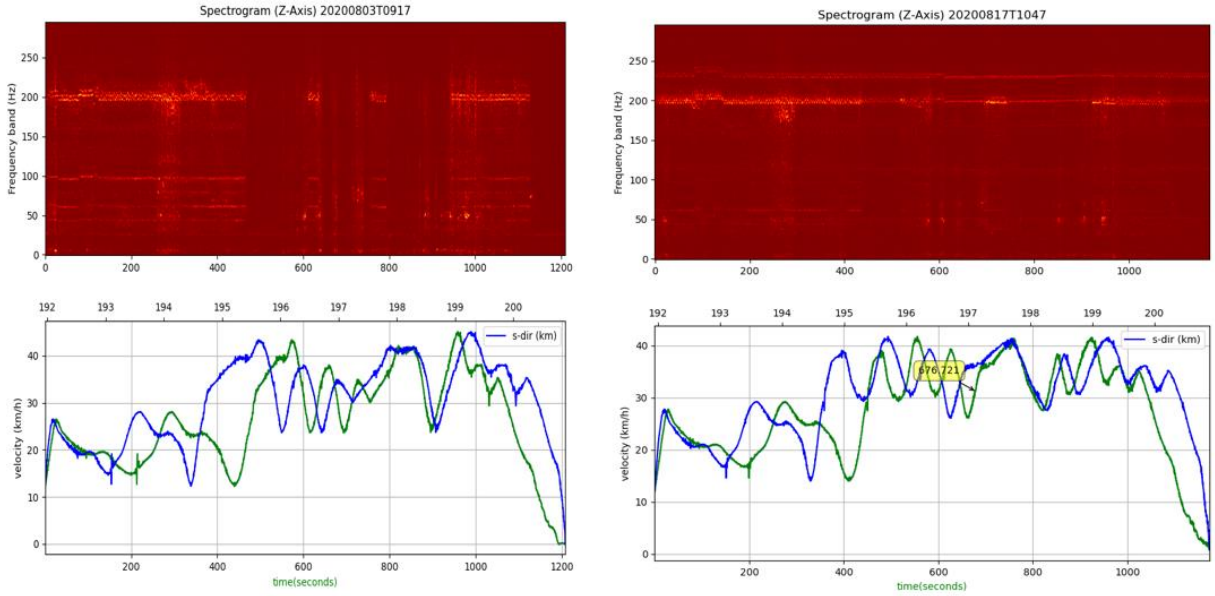

Figure 4.13 Experiment files 4 and 8, showing 'breaks' or up-down shifts along the otherwise consistent dominant frequencies depicted in Figure 4.12

Explanation as to what can cause the dominant frequencies to arise, and what parameters are required to use this information from spectrograms for chemometric analysis, is dived to in more next in the upcoming main chapters.

4.1.3 Referencing - Averaged Spectra

The same number of files, as was analyzed for individual spectra, were selected to produce the average spectra. It ought to be mentioned that the files in datafiles.py were carefully selected to begin with. Files that are clearly have exceptional information in the spectra or were start in exception, were saved in a different file variable list.

The averaged spectra were therefore constructed after visually inspecting more than the 23 files used in this study.

Figure 4.14, Figure 4.15 and Figure 4.16 shows (linearly) amplitude averaged spectra of x, y and z-axes respectively. A milder colormap is chosen to display the spectra, and the color bars are provided abreast for reference. A 3D surface plot is also plotted alongside spectra, since it gives the freedom to rotate the plot and the axes as wanted. 3D surface plots are also more useful when viewing the standard deviation spectra.

It must, however, be noted that the color change along the height of the 3D surface plot does not reflect the amplitude, although it does accentuate the high amplitude areas. Attempts were made to reflect the amplitude along the height of the 3D plot, but requires alterations and modifications to code that would take up much of the limited time available for analytical purposes of the study. Nevertheless, the amplitudes are still visible along the numerical axes to exact readings. Figure 4.14 and Figure 4.15 show the spectra for x and y axis, with the dominant frequencies standing out quite well. The band of vertical streak is comfortable visible in x-axis average spectrum. The 3D surface plot also reflects little noise along the data, as expected due to averaging effect.

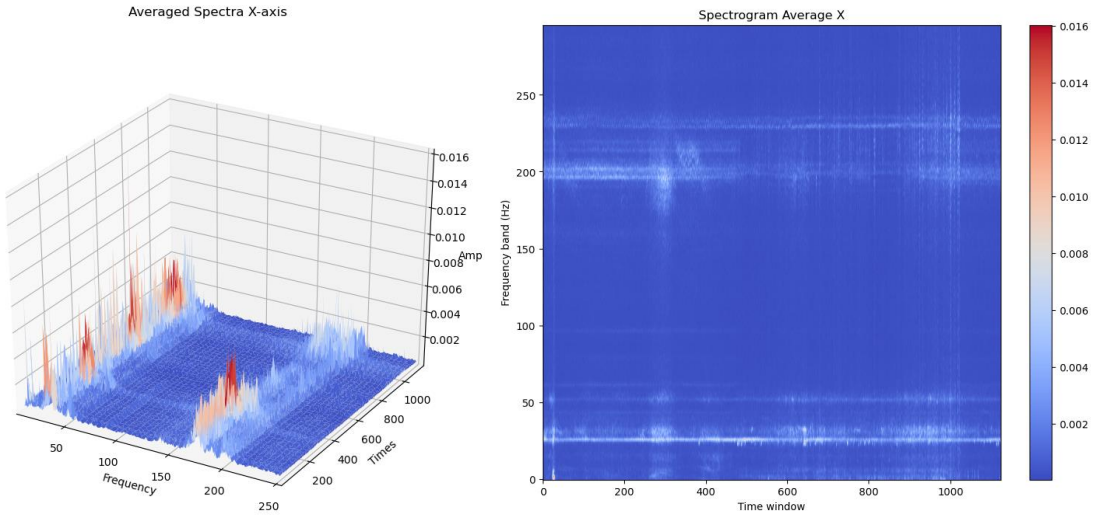

Figure 4.14 Averaged spectrum for X-axis, calculated over 17 files. Surface plot shown at left, and 2D spectrum at right

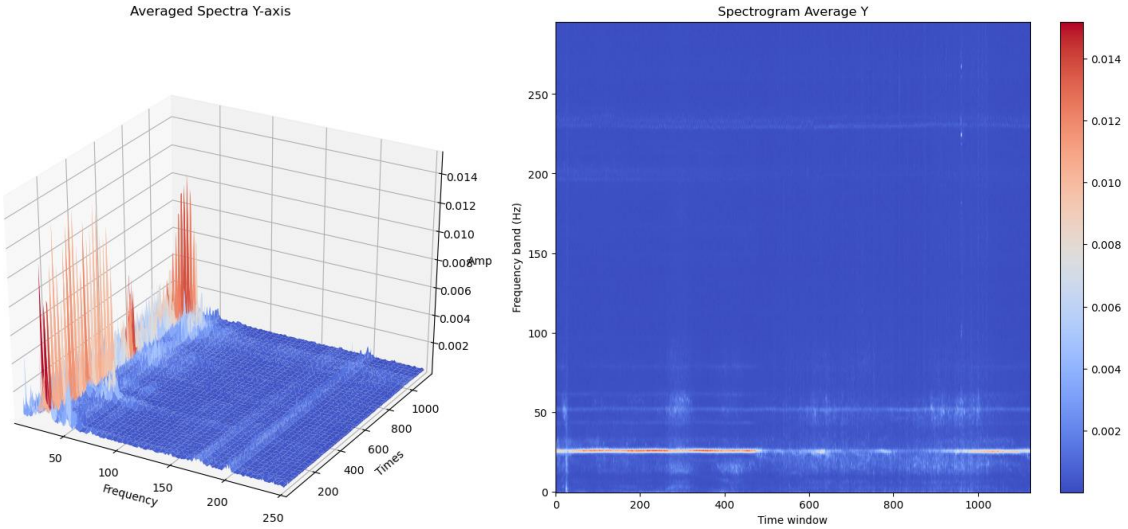

Figure 4.15 Averaged spectrum for Y-axis, with surface plot and 2D spectrum

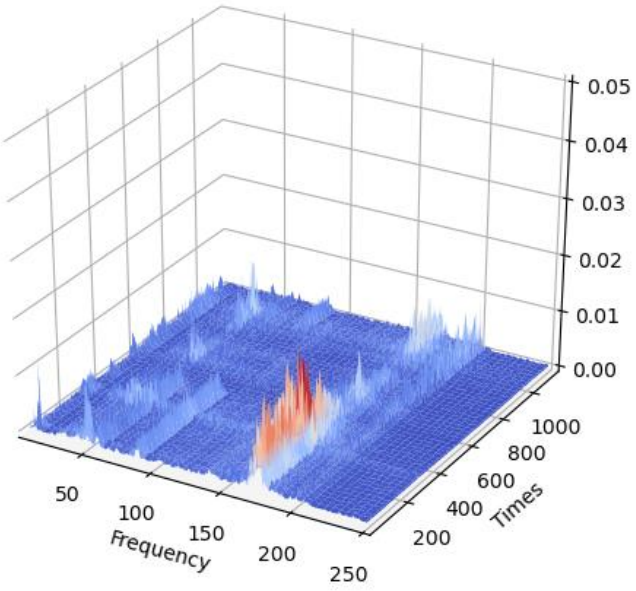

Figure 4.16 3D plot of averaged Z-spectrum

Figure 4.16 and Figure 4.17 are both averaged Z-spectrum, shown in separate figures. It is worth looking into the Z-spectra in greater detail since this direction is known to carry more important information related to track conditions and defects[7].

The 3D plot in Figure 4.16 shows a spectrum that also does not appear to have a noisy texture at the weaker frequencies. The active, dominant frequencies common throughout z-axis plots are clearly accentuated, with the characteristic bright frequency streak at the higher band of 150Hz standing out.

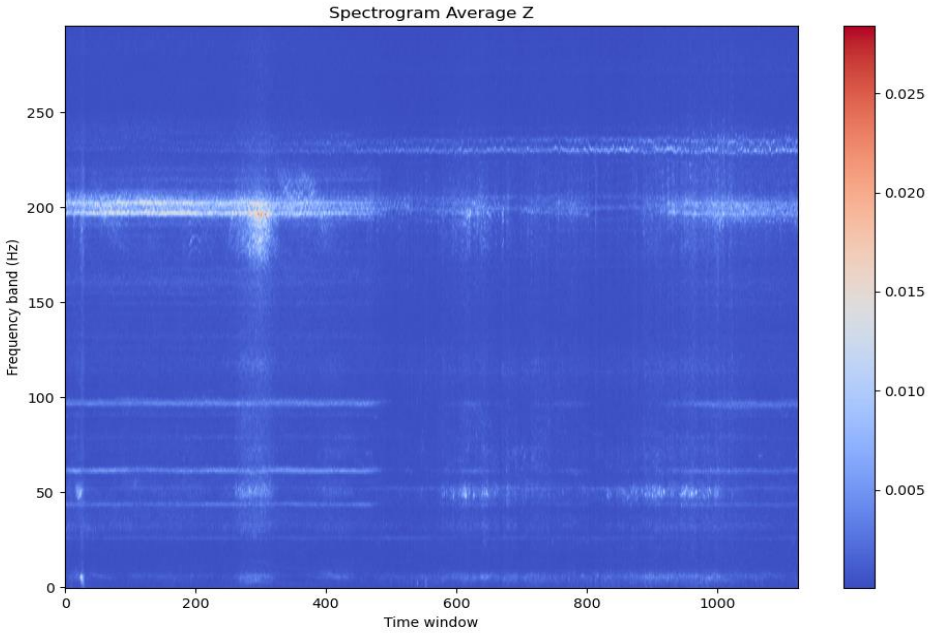

Figure 4.17 Spectrogram of averaged Z-spectrum

Figure 4.18 shows the previously mentioned set of individual spectra, as demonstration of some of the samples that were used to draw the average. The amplitude scale (z-limit in the plot) was kept constant, so it is *not* autoscaled according to individual spectrum amplitude values.

The comparison thus has sample spectrum that appears to overshoot the plot, such as the last plot in Figure 4.18.

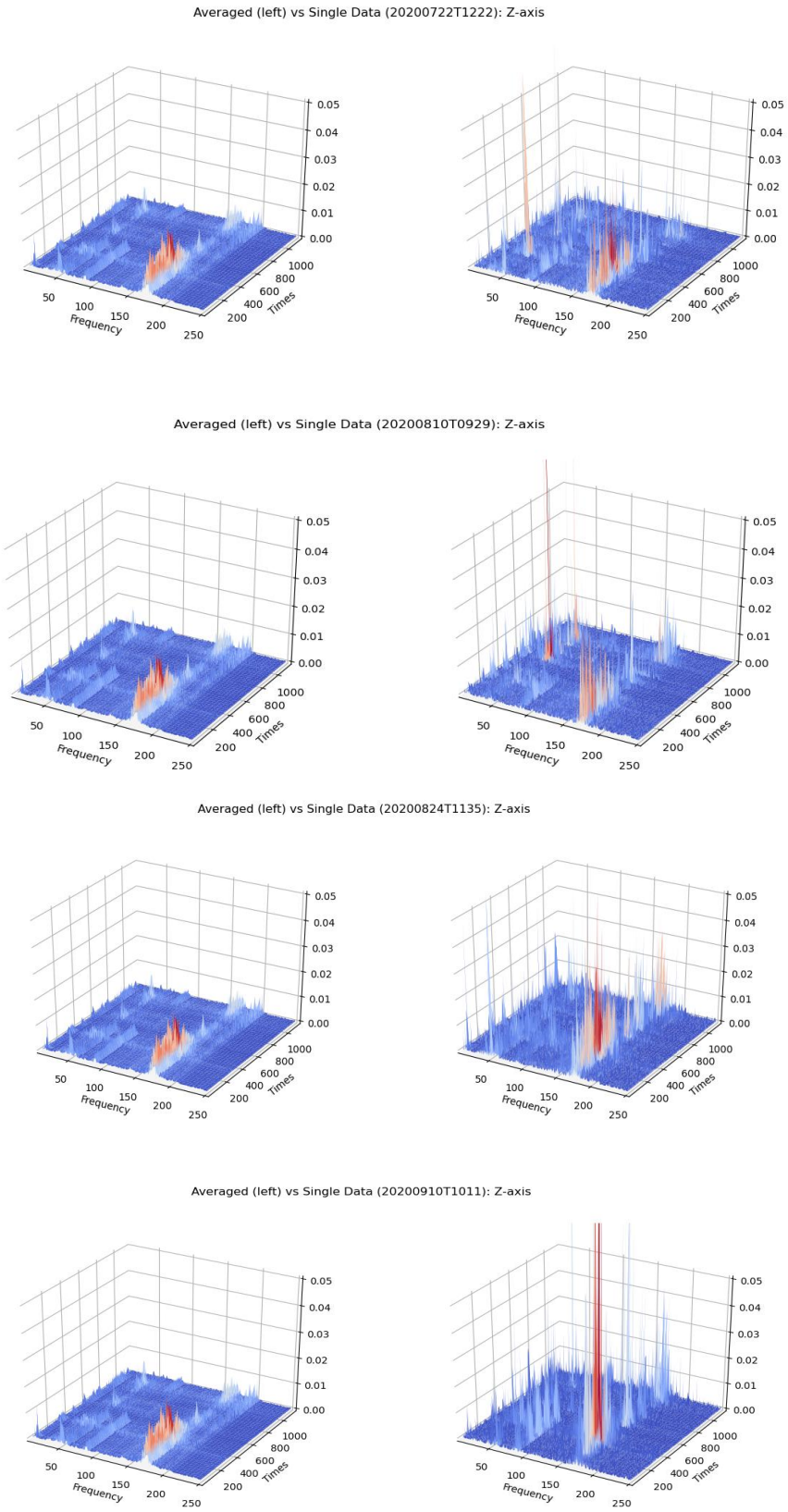

Figure 4.18 Averaged vs. Individual spectra

4.1.4 Visualizing Peak Variances - Standard Deviation Spectra

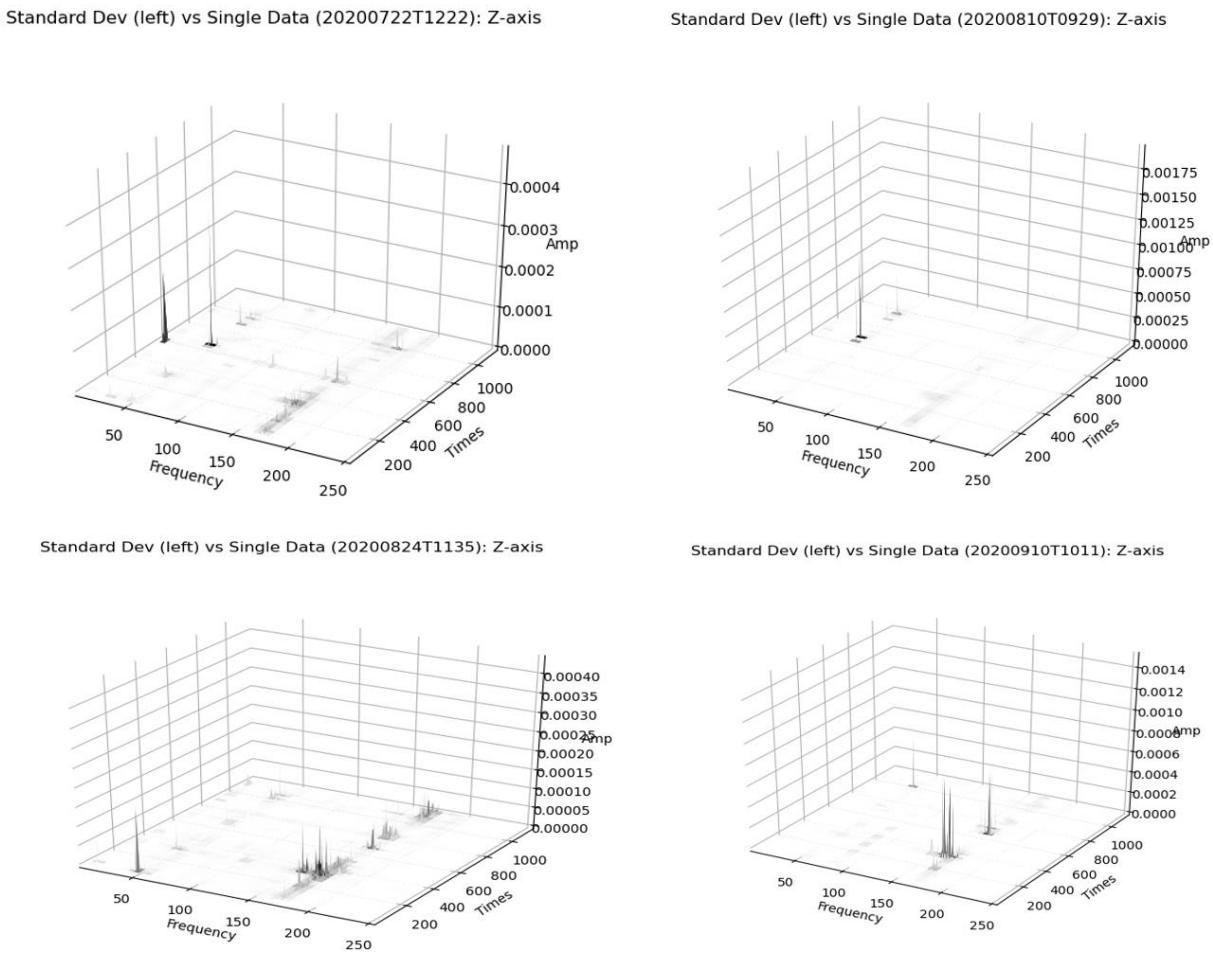

Figure 4.19 Variation in some of the sample spectra compared to mean spectra

Figure 4.19 shows the standard deviation spectra, where the amplitudes are calculated using the regular standard deviation formula.

The datasets used to calculate the standard deviation are part of the data used to calculate the average, so the average spectrum is not used as a reference against a new dataset in the plots here.

4.2 Chemometric Results – PCA

Figure 4.20 shows the results from PCA performed on the averaged Z-spectrum. Since it is not known how many PCs are needed to explain the variation amongst the data, the number of PCs was set to 12.

Scores and loadings are shown at the top row of the results in Figure 4.20. The results display samples and variables plotted along PCs 1 and 2. An Explained Variance plot at the bottom left shows how the 12PCs account for the variances in the dataset.

Scores:

Figure 4.21 shows the score plots along PC1-PC2, and PC1-PC3, at the right of the plot. Score plots were also checked across more PCs to see if any other PCs had an effect on the scores.

Loadings:

The loadings are similarly plotted for PC1, PC2 and PC3, shown in Figure 4.22, but were not easy to interpret at a glance. As recommended with PCA of spectral analysis[20], the loadings were plotted as line plots, which would mean looking at a particular 'acoustic spectrum' represented by that particular loading.

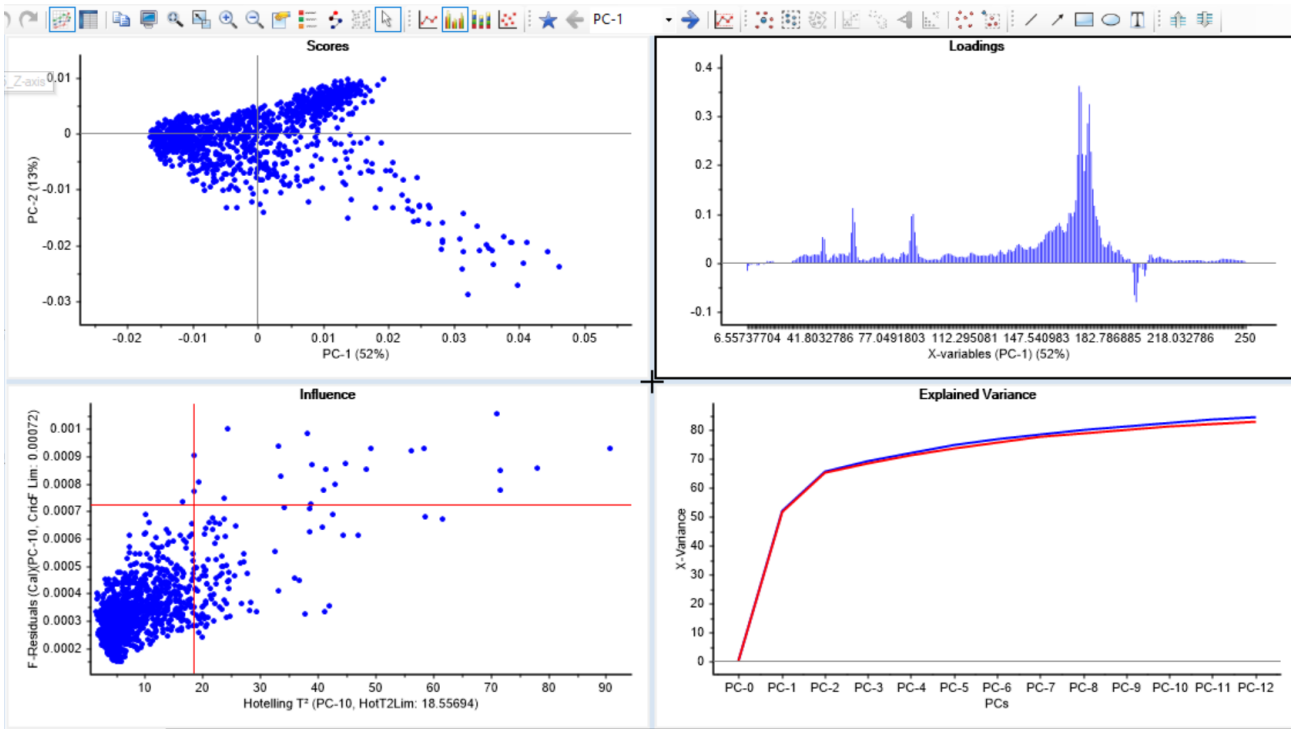

Figure 4.20 PCA Results – Average Spectrum – Z axis

Figure 4.23 shows the first 4 PCs as loading spectra. The remaining PCs vaguely resembled PC4, with distinct peaks, but very low percentage to account for variance.

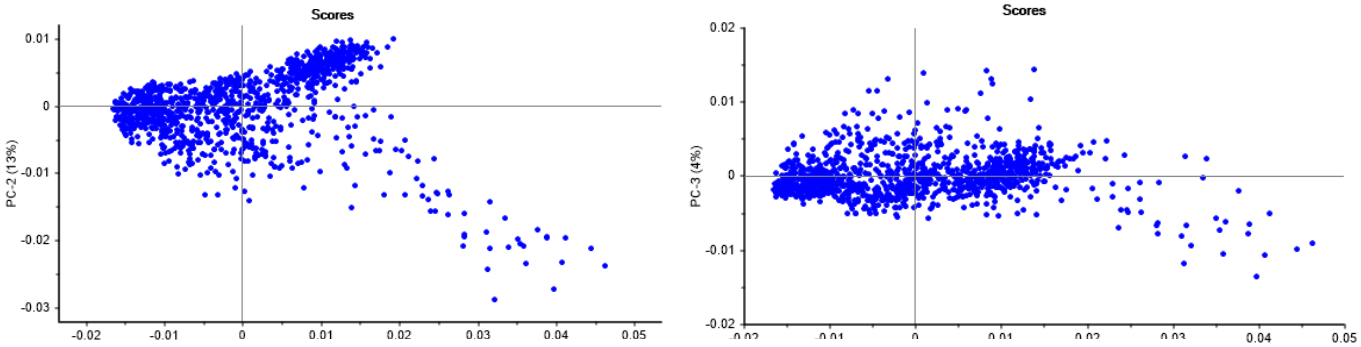

Figure 4.21 Score plots along PC1-PC2 space(left) and PC1-PC3 space (right)

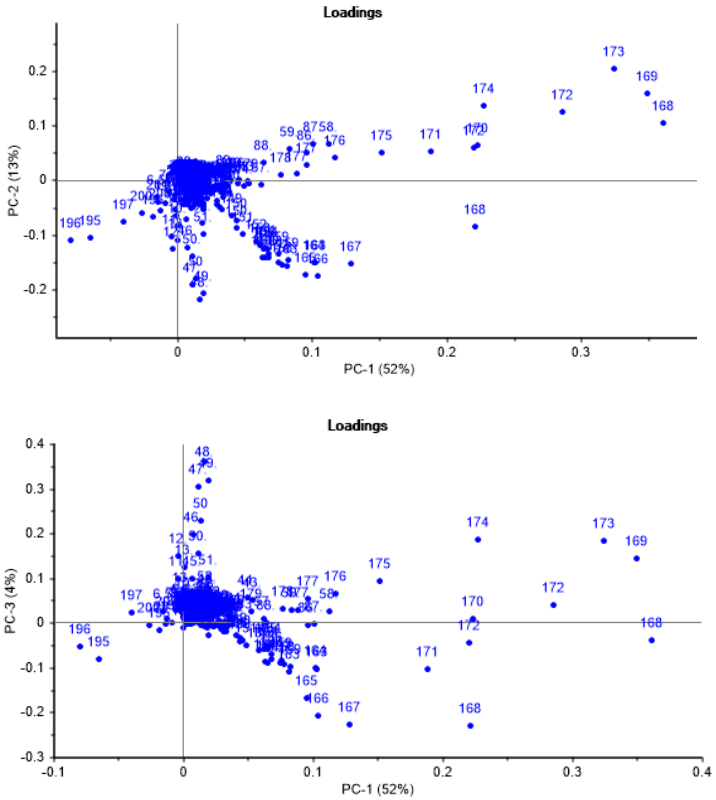

Figure 4.22 Loadings along PC1-PC2(top) and PC1-PC3(bottom)

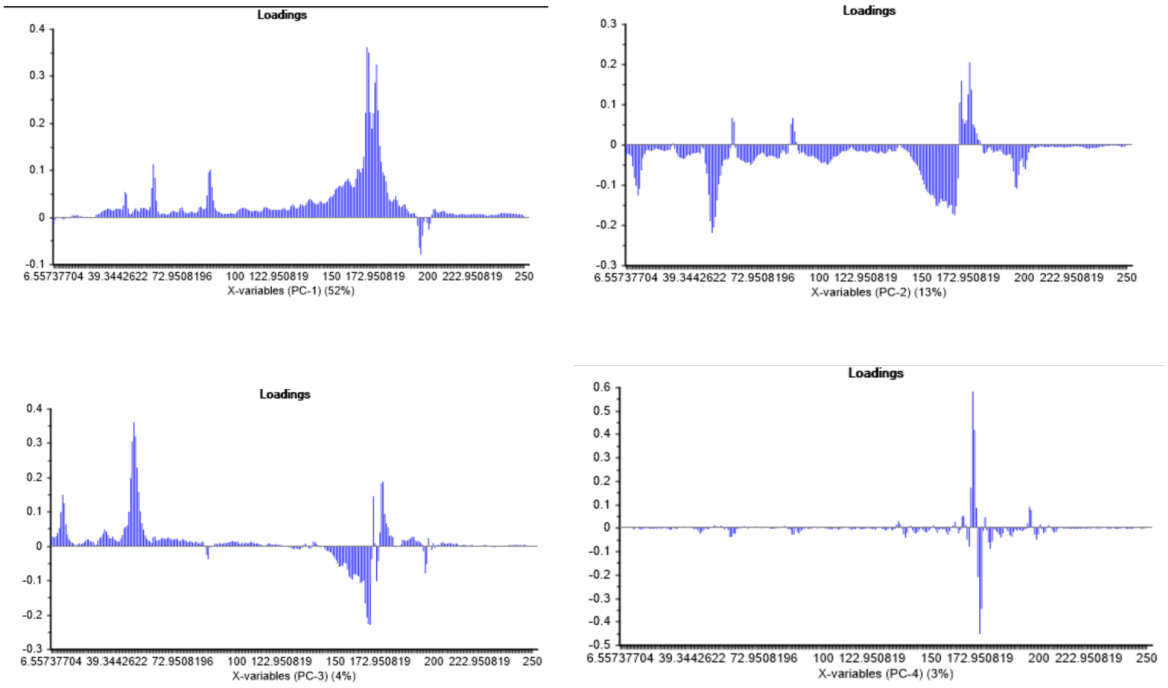

Figure 4.23 Loadings from first 4 PCs plotted as line plots.

5 Analysis

5.1 Spectral Analysis of Tri-axial Acoustic Data

Establishing frequency bands:

After observations from all spectra depicted in results, the following frequency bands are referred to for the rest of the analysis. The bands are within 250Hz, and not equal, rather, is sectioned to reflect the most recurring frequencies observable across a band. Therefore,

Low Frequency Band : 10Hz to 50Hz
Medium Frequency Band: 51Hz – 100Hz
High Frequency Band: 101Hz – 220Hz

Frequencies up to 5Hz have not been taken into consideration because they were already observed to have much higher intensities, and would have little significance given the conditions sought after in relation to the hypothesis, such as noises or defects generated along curved tracks, would usually be present at higher frequencies[6]

Common frequencies among all directions:

The averaged spectra of all the three axes, also found in Figures 4.14, 4.15 and 4.16 are compared since they are representative of all 17 datasets, and have pronounced dominant frequencies common across many experiments.

X and Z axis spectra have much of the structure in common, with both average spectra displaying two significant, high band frequencies of around 200Hz and 230Hz, present continually throughout the spectra. X and Y spectra, too, have common frequency bands in the lower range, of around 25Hz. Figure 5.1 shows a side-by-side shot of all 3 spectra.

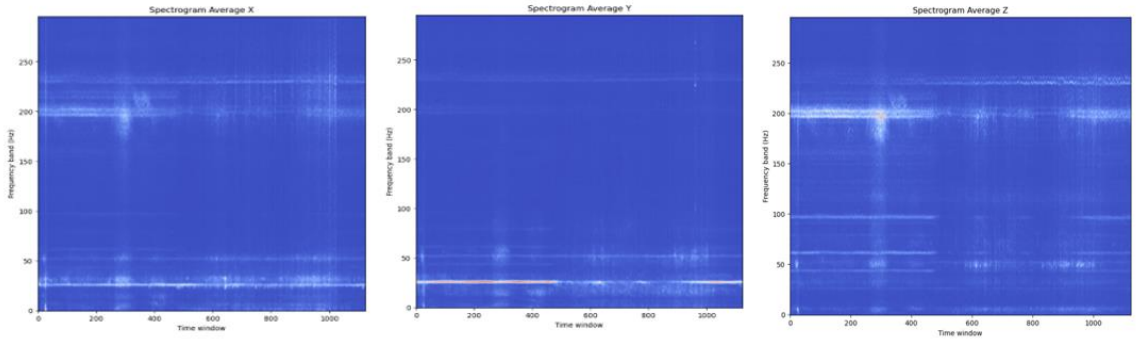

Figure 5.1 Average spectra of all 3 axes, with X spectrum sharing common frequencies with Z and Y spectra

Estimation or suggestion as to what contributes to these dominant frequencies are hard to offer without conducting proper experiments or modelling to find out what structures or rail-wheel dynamics constitutes these frequencies. However, an understanding of general acoustics and

spectrograms suggest that the harmonics appear as horizontal lines and as constant frequencies[25]. Some of these constant frequency bands, continuing at 50Hz, and 100Hz, as can be observed for Z average spectra, for instance, are also indicative of harmonics, and could arise due to structural vibration of the freight locomotive.

Bright, vertical streaks along frequency axes are also present on all 3 axes, although extremely vague in Y spectrum, seen in Figure 5.1, and is a feature deserving of further analysis. Although velocity of the vehicle was available, more information, such as the weight of the locomotive at the time of experiment, weight of the rail carriages attached to it, and some basic health checks of the rail tracks could solidify a better understanding of such patterns throughout the runs. Investigating velocity with acoustic data alone is not expected much using numerical methods.

Mean and Deviation Spectra: Comparing a new Z-axis spectrum with the averaged spectra:

A new, test spectrum is used to view results using the reference (averaged), Z-spectrum. Figure 5.2 shows the original z-spectrum from datafile name visible at the title of the figure. The test spectrum is observed to have quite high amplitudes at high frequency band.

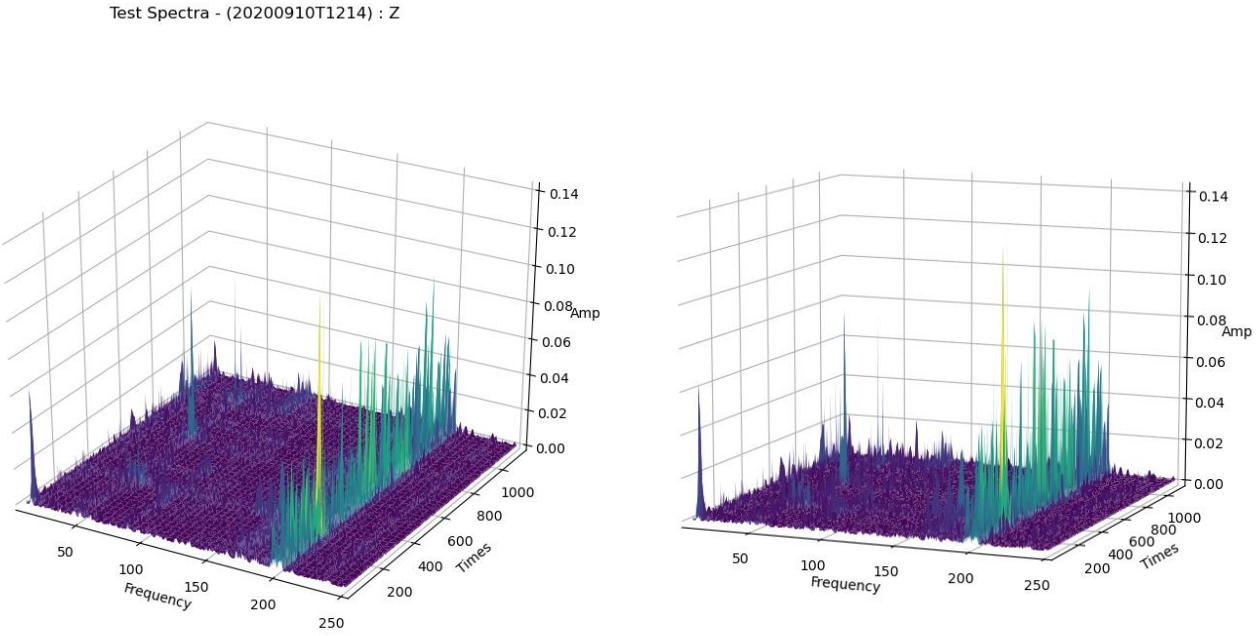

Figure 5.2 A new, test spectra, not used in prior analyses

Although the new data is referred as test spectra, there is no value tested yet per se. However, visual inspection can be done to observe if the reference spectra is representative of the new one. Figure 5.3 shows a comparison. The test spectrum appears unusually noisy because its amplitude axis is fixated with limits.

Figure 5.4 shows the standard deviation of the new dataset compared to the referenced spectrum. Upon observation, it can be said that the deviation is found mostly at higher frequency band, and not much in other areas, indicating the new test spectrum is not very far from the averaged one. The average spectra can thus be an acceptable reference to distinguish new data and note areas in spectra for further analysis.

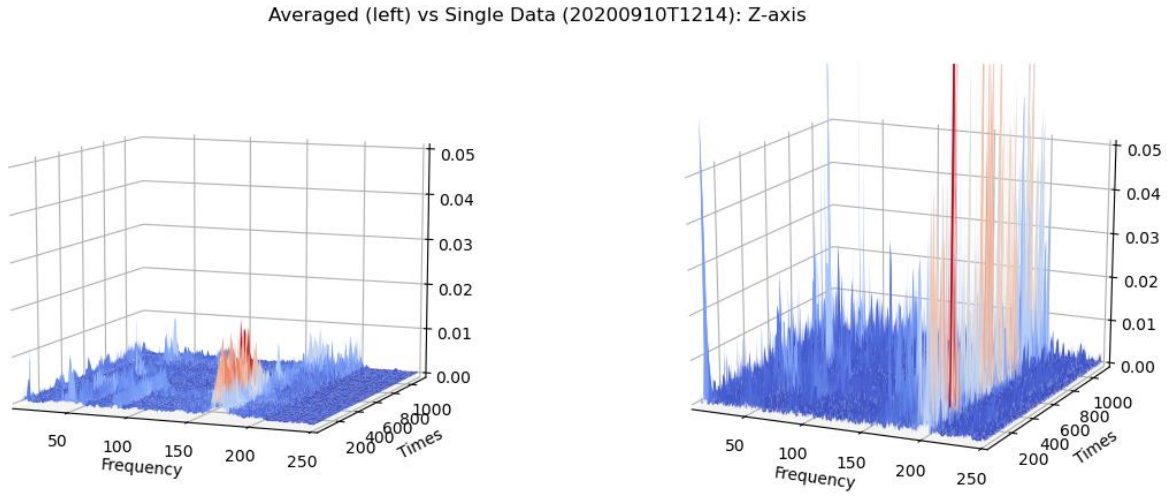

Figure 5.3 Average spectrum Vs. Test Spectrum

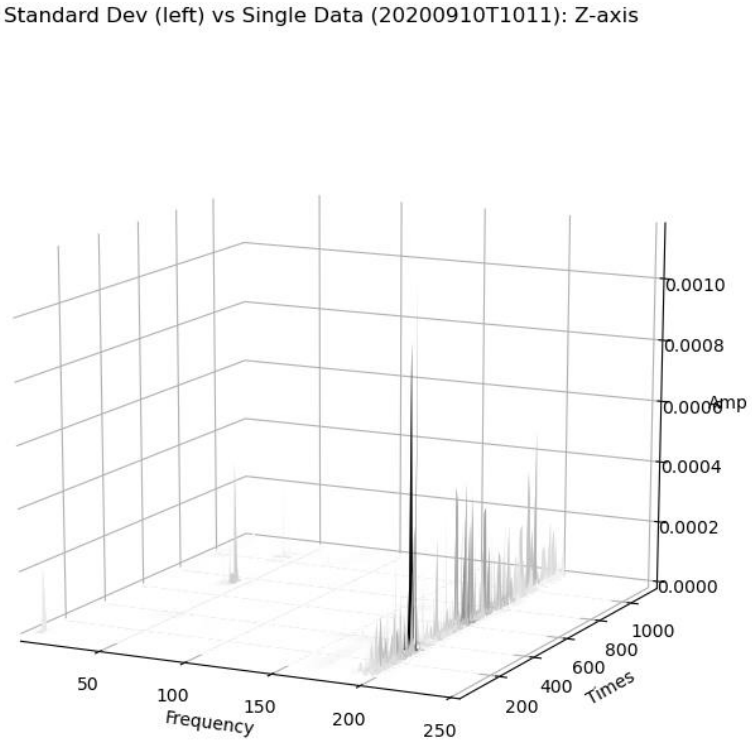

Figure 5.4 Standard Deviation spectrum from the newly compared data

5.2 Interpretation of Multivariate Data Analysis

Recalling Figure 4.20, the results revealed plots of PCA of averaged Z spectra, where the samples were essentially FFTs computed for the spectrogram. The score plots showed slight patterns towards PC1 and PC2, but when PC1 and PC3 were plotted, the scores showed no significant changed across PC3 component.

Observing Figure 5.5, which is the Explained Variance plot in numerical view, PC2 can be seen to account for 65% of the variance, and PC5 accounted for 1/3rd of it.

The loading plots were also revealed in Figure 4.22 and Figure 4.23, but can hardly be interpreted at this stage without understanding what contributes to the frequencies that the loadings constitute of.

Explained X		PC-0	PC-1	PC-2	PC-3	PC-4	PC-5
		1	2	3	4	5	6
Calibration	1	0.0000	52.2027	65.5871	69.2988	72.2381	74.7083
Validation	2	0.0000	51.7917	65.0815	68.5970	71.3999	73.7543

Figure 5.5 Explained Variance – numerical view

What does the PCA results mean for an averaged spectrum?

As an unsupervised algorithm, PCA itself is a method that will organize any data according to a parameter explaining differences in that data. For the averaged Z spectra, the best a PCA can reveal is the combination of frequencies that have changed most throughout an average day of the locomotive in its track on Brevikbanen. This analysis is very far from being able to identify what is unusual about the rail-wheel dynamic, but has still produced a 'signature' of Principle Components that can apparently account for half the variation in the time-sequenced FFT.

However, when assuming PCA analysis for extracting features from spectral data, this approach is not the recommended one. For an acoustic monitoring system sought to identify and locate rail structure and vehicle structure defects, these FFTs would have to be studied and sorted for particular time segments, where interesting developments in amplitudes lie. Therefore, instead of using consecutive FFTs from spectrum, they would have to be selected based on unusual activity, or by using averaged and deviation spectra to find out interesting arenas, as is suggested in previous chapters.

Some analysis was attempted to isolate FFTs from a number of individual spectral data instead of a single averaged one, but the analysis yielded anomalous results, which indicated making improvements to the segmentation of time-signal data – resulting in halted attempts given the scope and limitations of the study.

6 Discussion

Much of the performed analysis proposed in this study have an indistinct structure, and has been lacking numerical definition for quantifying the analysis. Denoting dominant frequencies and velocity changes, for example, were done mostly on visual observations. While visual interpretation has largely a role in interpreting chemometrics results, many of the analytical approach have room for improvement that require more time and some much in-depth understanding of data manipulation – a lot of which cannot be done in the span of a semester, especially given the pre-existing, minimal set of data to work with.

A lack of reference data:
Although unsupervised means are available for starting phase chemometrics, in order to be able to use acoustic chemometrics to a more rigorous degree, reference data have to be established for more supervised analyses, either by mathematical modelling or by experimental means.
Many literature have been overviewed to observe what category of experiments and dynamic modelling studies have been done, and there indeed has been a number of studies where wheel squeal and effect of flanging on curves have been experimented with in roller rigs[6], with findings suggesting, for instance, that high squealing us likely to occur if the ratio of the axle distance to the curve radius is 100 or less. The results from this extensive study also confirmed that curve noise occurs at the natural frequency of the wheel, squealing occurs at high frequencies and flange noises occur in various modes. The methodology used in this study was to observe the frequency response upon hammer impact. Studies conducted with objective to improve ride quality and reduce the effects of vibrations [26] have also attempted to simulate track irregularities. Finite element model and graphic modelling using CAD were done in one of the studies in order to develop a rail vehicle model that takes into account interactions with other connected structures of the vehicle[27].

A schematic overview of these papers was suggestive of many ways of modelling effects and interaction of a vehicle rolling on a rail. The suggestions could be studied more to find ways to model the hypotheses and track dynamics to be finally used for calibration and validation in chemometric analyses.

Analytical methods
Tracking of spectra to the corresponding map containing track data could use improvements and much less chaotic way of tracing spectrum data to the location, but devising a code for just this one feature would have meant investing a large amount of time studying functions and libraries of Python, which was not to be the focus of the analysis. Thus, even though the method requires a careful guidance between plots, was kept as is. This analysis method can for sure be made much simpler.

Different sampling rates
Acoustic data and vehicle velocity data were also sampled at different rates, which posed a problem velocity data was attempted to be included in chemometric analysis. The 5Hz data could have been interpolated to fill 500Hz sampling, but would again require time to create a proper code before any analysis can begin. However, attempts were still made to gather 5Hz velocity data to fit into the spectrum matrix (X data matrix), but proved inefficient and time consuming.

Improvements

It is also worth discussing that simple averaging formula were used to compete amplitude averages, but this method would have to be changed when working with new data, in which case exponential averaging is recommended, which should give more weights to newer data. Filtering and replicates averaging were not included as part of methodology, since the CDC is not reported to have any low-pass filters in it.

Any further studies carried on this topic is urged to re-conduct planned experiments with proper sampling rates, filtering, static data monitoring - and ensure that the needful data processing steps are in place to obtain informative, quality data for analysis.

7 Conclusion

The thesis has explored frequency analysis and primary multivariate analysis to study the potential of acoustic chemometrics on pre-existing acoustic data from IMU measurements. The goal of the study was to observe the frequency spectra along a vehicle's runtime to see if the frequency content was indicative of diagnosing anything out of the ordinary in a time-varying process.

The frequency bands from all three axes were noted to get an initial understanding of the dominant frequencies existing along all axes. analyzed and patterns along the spectra were visually observed to extract areas or information that can be used for further specific analysis. Average spectra were also studied to get a much precise understanding of the existent frequencies along the three orthogonal axes. Similar frequency bands were observed among all three axes along 25Hz, 50Hz and 100Hz, explainable by the concept of harmonic frequencies which occur at multiples of fundamental frequency.

Velocity and s-direction data were observed to see if a pattern emerges when velocity is compared to spectra, and if interesting pattern can be traced back using s-direction data using GPS coordinates. Using the s-direction reference, the section of track where streaks appeared along all axial spectra was identified, and is worth investigating further into.

Mean and standard deviation spectra were generated for all axes, but analyzed for z-axis only. Comparison showed that the averages spectra well represented spectrum of any given dataset, which was tested with a newly imported dataset not used for calculation of mean spectra. The standard deviation plots helped protrude areas where the amplitudes stood out compared to the averaged spectra, and could be a decent starting point for analysis at the absence of proper reference data to draw chemometric (regression) analysis with.

Shortcomings and limitations of the study were brought into light and discussed, along with examples of a few studies that illustrate how rail-wheel modeling can be done and what these modelling and experimental results can be used for.

New, planned experiments with a more controlled and informative method is suggested.

8 Future Works

So far, FFT has been applied to time series data, it has been scrutinized for not retaining information about time[28], but rather as a function of position. A study on Condition-Based Monitoring has also challenged FFTs abilities in being used for fault detection and diagnosis, stating FFTs indication of harmonics, where there should be in presence of defects, shows how FFT treats the "change of vibration signal from sinusoidal to something twisted or flattened"[29].

The time-series analysis method that is more often suggested in replacement of FFTs is wavelet-based transform. A more detailed study of this transform for signal analysis is available in the research article noted in this reference[30]. This analytical approach is reported to display both time and frequency localization very well, which would be nothing short of advantageous given the study at hand. Further study of this algorithm for frequency analysis is highly recommended.

An IEEE paper published back in 1997, alternatively, suggested FFTs based on wavelet-based transform, which could be another possibility worth testing out.

A machine learning approach that involves use of 'Deviation Networks'[31], for anomaly detection in absence of volumes of labelled data is also recommended, as it has potential to be applied in fault identification analysis with very few classified or labelled data. This method is, of course, relevant in the more advanced stages of acoustics study from now, however, this method has come forth with promising results that shows better anomaly-scoring in comparison to its counterparts, and should very well be worth studying.

References

[1] H. OUFERROUKH, ‘European Rail Traffic Management System (ERTMS)’, *ERA*, Sep. 10, 2018. https://www.era.europa.eu/activities/european-rail-traffic-management-system-ertms_en (accessed Jun. 01, 2022).

[2] ‘Rail and waterborne — best for low-carbon motorised transport — European Environment Agency’. https://www.eea.europa.eu/publications/rail-and-waterborne-transport (accessed Jun. 01, 2022).

[3] Y. Zhao, X. Ling, Z. Wang, W. Gong, and G. Li, ‘Acceleration Frequency Characteristics of the Freight-Train-Induced Vibration of the Beijing-Harbin Railway Subgrade’, *Shock Vib.*, vol. 2020, pp. 1–11, Nov. 2020, doi: 10.1155/2020/6651713.

[4] D. Milne *et al.*, ‘Proving MEMS Technologies for Smarter Railway Infrastructure’, *Procedia Eng.*, vol. 143, pp. 1077–1084, Jan. 2016, doi: 10.1016/j.proeng.2016.06.222.

[5] J. Majala, *Frequency analysis of accelerometer measurements on trains*. 2017. Accessed: Nov. 16, 2021. [Online]. Available: http://urn.kb.se/resolve?urn=urn:nbn:se:ltu:diva-63930

[6] J. Kim, Y. Yun, and H.-M. Noh, ‘Analysis of Wheel Squeal and Flanging on Curved Railway Tracks’, *Int. J. Precis. Eng. Manuf.*, vol. 20, Sep. 2019, doi: 10.1007/s12541-019-00225-7.

[7] T. Abuhamdia, S. Taheri, A. Meddah, and D. Davis, *Rail Defect Detection Using Data From Tri-Axial Accelerometers*. 2014. doi: 10.1115/JRC2014-3703.

[8] ‘Materiell - Grenland Rail’. http://www.grenlandrail.no/?CatID=1180 (accessed May 26, 2022).

[9] J.-P. Polizzi, B. Fain, and F. Maspero, ‘Chapter 45 - Accelerometer’, in *Handbook of Silicon Based MEMS Materials and Technologies (Third Edition)*, M. Tilli, M. Paulasto-Krockel, M. Petzold, H. Theuss, T. Motooka, and V. Lindroos, Eds. Elsevier, 2020, pp. 879–898. doi: 10.1016/B978-0-12-817786-0.00045-1.

[10] ‘2.5: Spring-Mass Oscillator’, *Physics LibreTexts*, Aug. 08, 2019. https://phys.libretexts.org/Courses/University_of_California_Davis/UCD%3A_Physics_7A_-_General_Physics/02%3A_Applying_Models_to_Mechanical_Phenomena/2.05%3A_Spring-Mass_Oscillator (accessed Jun. 01, 2022).

[11] N. C. Yoder and D. E. Adams, ‘3 - Commonly used sensors for civil infrastructures and their associated algorithms’, in *Sensor Technologies for Civil Infrastructures*, vol. 55, M. L. Wang, J. P. Lynch, and H. Sohn, Eds. Woodhead Publishing, 2014, pp. 57–85. doi: 10.1533/9780857099136.57.

[12] A. Venkatanarayanan and E. Spain, ‘13.03 - Review of Recent Developments in Sensing Materials’, in *Comprehensive Materials Processing*, S. Hashmi, G. F. Batalha, C. J. Van Tyne, and B. Yilbas, Eds. Oxford: Elsevier, 2014, pp. 47–101. doi: 10.1016/B978-0-08-096532-1.01303-0.

[13] F. J. Harris, ‘Chapter 8 - Time Domain Signal Processing with the DFT’, in *Handbook of Digital Signal Processing*, D. F. Elliott, Ed. San Diego: Academic Press, 1987, pp. 633–699. doi: 10.1016/B978-0-08-050780-4.50013-8.

[14] R. Oshana, ‘4 - Overview of Digital Signal Processing Algorithms’, in *DSP Software Development Techniques for Embedded and Real-Time Systems*, R. Oshana, Ed. Burlington: Newnes, 2006, pp. 59–121. doi: 10.1016/B978-075067759-2/50006-5.

[15] ‘Spectral Leakage’. https://www.physik.uzh.ch/local/teaching/SPI301/LV-2015-Help/lvanlsconcepts.chm/Spectral_Leakage.html (accessed May 26, 2022).

[16] ‘Understanding FFTs and Windowing’. https://www.ni.com/en-no/innovations/white-papers/06/understanding-ffts-and-windowing.html (accessed Jun. 01, 2022).

[17] ‘Spectrogram using short-time Fourier transform - MATLAB spectrogram - MathWorks Nordic’. https://se.mathworks.com/help/signal/ref/spectrogram.html (accessed May 27, 2022).

[18] ‘scipy.signal.spectrogram — SciPy v1.8.1 Manual’. https://docs.scipy.org/doc/scipy/reference/generated/scipy.signal.spectrogram.html (accessed May 29, 2022).

[19] K. H. Esbensen, B. Hope, T. T. Lied, M. Halstensen, and K. Sundberg, ‘ACOUSTIC CHEMOMETRICS FOR FLUID FLOW QUANTIFICATIONS—II: A SMALL CONSTRICTION WILL GO A LONG WAY’, p. 29, 1999.

[20] K. H. Esbensen, D. Guyot, F. Westad, and L. P. Houmoller, *Multivariate Data Analysis: In Practice : an Introduction to Multivariate Data Analysis and Experimental Design*. Multivariate Data Analysis, 2002.

[21] ‘Brevikbanen’. https://skinnelangs.no/index.php?line=37 (accessed May 29, 2022).

[22] N. F. Güler and S. Koçer, ‘Classification of EMG Signals Using PCA and FFT’, *J. Med. Syst.*, vol. 29, no. 3, pp. 241–250, Jun. 2005, doi: 10.1007/s10916-005-5184-7.

[23] H. Rahman, M. Ahmed, and S. Begum, *Non-Contact Physiological Parameters Extraction Using Camera*. 2015.

[24] D. Pelliccia, ‘Classification of NIR spectra using Principal Component Analysis in Python’, Mar. 23, 2018. https://nirpyresearch.com/classification-nir-spectra-principal-component-analysis-python/ (accessed May 30, 2022).

[25] ‘Fundamental frequency and harmonics’. https://homepage.ntu.edu.tw/~karchung/phonetics%20II%20page%20eight.htm (accessed Jun. 01, 2022).

[26] Y. Fan and W.-F. Wu, ‘Dynamic Analysis and Ride Quality Evaluation of Railway Vehicles – Numerical Simulation and Field Test Verification’, *J. Mech.*, vol. 22, Mar. 2006, doi: 10.1017/S1727719100000721.

[27] R. MacNeill and G. Gough, *Predicting the Natural Frequency of Train Structures Using Detailed Finite Element Models*. 2016. doi: 10.1115/JRC2016-5835.

[28] S. Alwadi, M. T. Ismail, and A. P. T. D. S. A. Abdul Karim, ‘A Comparison Between Haar Wavelet Transform and Fast Fourier Transform in Analyzing Financial Time Series Data’, *Res. J. Appl. Sci.*, vol. 5, May 2010, doi: 10.3923/rjasci.2010.352.360.

[29] D. Baglee, E. Jantunen, I. El-Thalji, and T. Lagö, *Problems with using Fast Fourier Transform for rotating equipment: Is it time for an update?* 2014. doi: 10.13140/2.1.2679.1363.

[30] N. C. F. Tse and L. L. Lai, 'Wavelet-Based Algorithm for Signal Analysis', *EURASIP J. Adv. Signal Process.*, vol. 2007, no. 1, p. 038916, Dec. 2007, doi: 10.1155/2007/38916.

[31] G. Pang, C. Shen, and A. van den Hengel, 'Deep Anomaly Detection with Deviation Networks', arXiv, arXiv:1911.08623, Nov. 2019. doi: 10.48550/arXiv.1911.08623.

Appendices

Appendix A **Thesis Task Description**

University of South-Eastern Norway

Faculty of Technology, Natural Sciences and Maritime Sciences, Campus Porsgrunn

FMH606 Master's Thesis

Title: Real time monitoring of train wheels and track conditions based on acoustic measurements and multivariate data analysis

Assess acoustic chemometrics potential to detect and predict conditions related to train's infrastructure, especially the train's wheels and the track.

USN supervisor: Maths Halstensen

External partner: Per Ivan Januschas, CEMIT Digital Porsgrunn, Norway

Task background:

Acoustic chemometrics

Chemometrics is the science that traditionally deals with data-driven extraction of information from chemical systems. Chemometrics is a basic intradisciplinary field that makes use of multivariate stochastic methods, applied mathematics, computer science and traditional computer science to address problempositions inchemistry, biochemistry, medicine and process industry. It has been shown that the same methods also have application in other more traditional forms of engineering such as construction, construction, mining, processing plants, predictive maintenance, etc. And by using the same methods as in data-analytical disciplines we will be able to use acoustic chemometrics to extract information from all material types such as liquids, gases and solids to derive information in the same way as the aforementioned disciplines

CEMIT Research/Product Development Project for Acoustic Chemometrics

Broken rails

Bane Nor intends to roll out the European Rail Transport Management System (ERTMS) in Norway during the period of 2021-2034. This, in short, means a transition to a digital signal system with no further use of the existing signaling system. The information will be sent directly to the train drivers console inside the train via a dedicated GSM-R system (GSM-R is a mobile phone system reserved for communication within the rail industry).
This means that the principle of a closed circuit, which used in today's existing signaling system will no longer be available to analyze the track for breakage in the rails.
CEMIT wants to look at whether it is acceptable to investigate this using acoustic chemometrics. We believe that this is a good potential for this technology to detect and predict the distance between a train and a rail break, and where acoustic chemometrics will be used to investigate if there is actually a break in the track by analyzing the actual sound emitted as a result of a train wheel rolling on the track.

«Screaming rails»

CEMIT also has proposed a theory that acoustic chemometrics can be used to look at causal relationships that cause rolling stock to create "wailing rails" in some cases. In tight turns, this will be "sort of normal" since the friction between the flange of the wheel and the rail increases at the entrance to a sharp curve. But what could be the reason why the train makes such noise even in wider curves? CEMIT wants to look at the total data that such a soundscape creates to see if something stands out, and whether acoustic chemometrics are suitable for analyzing these relationships. We will therefore look at whether we can isolate deviations in rail/train wheels that together produce this undesired soundscape. This can have a number of different causes, but e.g. bogie geometry that is not 100% aligned with the rail aisle may cause the wheels to constantly be left at the wrong angle to flange, thereby increasing wear and tear, or the wheel axle may be subjected to geometric travel, which in addition will cause vibrations in the train that will cause negative effects for the infrastructure, rolling stock and passengers.

Rolling stock wheels wear & tear

Furthermore, CEMIT recognizes that a train wheel in use wears out. Therefore, over time, the circumference of the wheel decreases. There are set criteria for the permissible minimum and maximum wheel diameter. At CEMIT we have therefore formulated a hypothesis that when the wheel wears down, the frequency and amplitude height will change quite noticeably. If this entails any level of correctness, CEMIT also hypothesizes that one will be able to real-time analyze this sound, and thus have a good data basis for predicting the remaining wheel life up to the next overhaul of the wheel, and likewise the remaining lifetime in total. The section on "screaming rails" mentions several of the causes of wear and tear, and also several of the consequences this may lead to.

Damage to/breakage in wheel/material fatigue/un-roundness/wheel profile/wear & tear og bearings and brakes

In the same way that a wheel that wears gradually will change its frequency, this change is likely to occur if the wheel is subjected to other changes over time, especially with sudden changes. CEMIT has formed a hypothesis that all these various influences on the wheels will have an acoustic "overall picture" and that by analyzing the sound these conditions will create, we will be able to distinguish them, isolating each individual condition. With this as a starting point, as a theory it will only be our imagination that limits what we can find. This will require an effort in the way of mathematical modelling, but not to the extreme in the context of engineering.

Other potential applications

- Listening to power loads drawn at the railway switching machines.
- Possible tools REW Room Equalizing Wizard. Real Time Analyzer.
- Potential source of information: GKN – They are using has predictive maintenance with the extraction of vibrations and acoustics for predictive analysis
- More information can be found by searching for "predictive analysis and maintenance"

It is aspired that good results based on this project will lead to peer-reviewed publication in an academic journal and the student group will be co-authors of the publication.

Task description:

Academic approach

One approach will be mostly academic in nature, and involve the University of South-Eastern Norway in Porsgrunn that will provide research assistance resource(s) and miscellaneous technical equipment. Some equipment will need to be acquired by CEMIT Digital. A list of suggested equipment can be found further down in this document.
A description of the data harvesting methods will be developed as part of the students' project work.
The data the student collects will be analyzed to find areas in the data collection that stands out for further and more specialized data harvesting and further specific analysis.

Expected result

The analysis of data will hopefully show that we can manage to isolate frequency and amplitude areas in the collected material that subsequently can be related to the hypotheses. From this we will develop data algorithms to perform real-time analysis on incoming data in the specific areas, and send the result, for example, directly to train drivers in cases such as detected rail breakage. If successful, the technology required to achieve this will be integrated into the CEMIT product IMU+CDC (Inertial Movement Unit + CEMIT Data Collector)
The scientific approach will be emphasized and will be presented in the form of a scientific article, which we wish to present at the SIMS conference the same year. CEMIT will, together with the student and Professor Maths Halstensen, be responsible for the preparation of the data and authorship of this article.

Data harvesting

- Installation of accelerometer on wheel shafts
- Installation of accelerometer inside the cockpit of a train
- Installation of accelerometer inside passenger cabin on a train
- Logging data to the CDC

Signal processing

- Sensor with sample rate 300kHz
- FFT per 4096 samples is stored on disk - assumed 70 Hz
- Post-processing with filter or non-causal mean
- Spectra are stored together with GPS position mtp. geo-location of the measurement.
- Spectra is presented as sonogram.
    - 3D plot over spectra in chronological order
    - Plots made also in kilometeration axis

Equipment

Hardware

- 3-axis accelerometer for measurements in X,Y and X plane
- Analog and UL microphone sensors (connected to CDC and/or industrial pc)
- NI-DAQ ADC box with USB, power supply and optionally. Signal Amplifier
- A powerful log/post-processing industrial PC (oversized for computing power RAM/DISK/CPU)

Publishing

It is aspired that the results based on this project will lead to peer-reviewed publication in an academic journal and the student will be co-authors of the publication.

Student category: IIA student

The task is suitable for online students (not present at the campus): No

Practical arrangements:

Supervision:
As a general rule, the student is entitled to 15-20 hours of supervision. This includes necessary time for the supervisor to prepare for supervision meetings (reading material to be discussed, etc).

Signatures:

Supervisor (date and signature):

Student (write clearly in all capitalized letters):
DILRUBA TARIQ JINIA

Student (date and signature):
31st May 2022

Appendix B **GitHub link for all Python source codes**

[GitHub Source Codes]

Appendix C **GitHub link for all Python source codes**

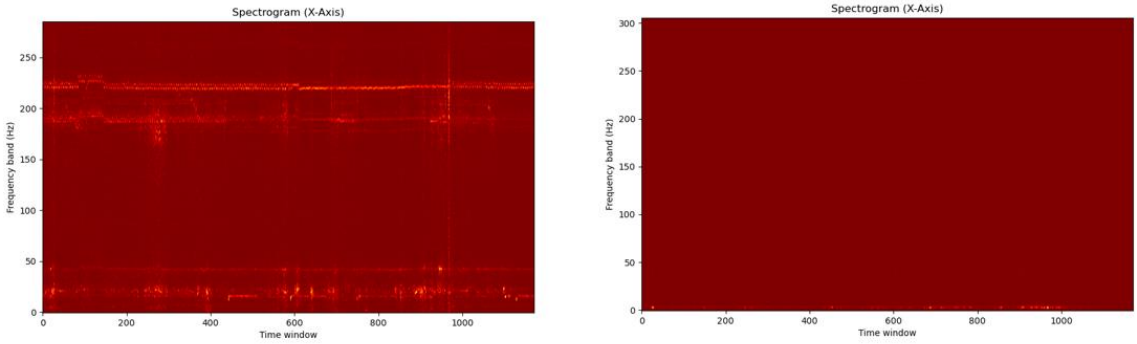

(Left) Spectrum without the initial low frequencies (Right) Spectrum will all frequencies